

Mixture of Many Zero-Compute Experts: A High-Rate Quantization Theory Perspective

Yehuda Dar

Faculty of Computer and Information Science, Ben-Gurion University

YDAR@BGU.AC.IL

Abstract

This paper uses classical high-rate quantization theory to provide new insights into mixture-of-experts (MoE) models for regression tasks. Our MoE is defined by a segmentation of the input space to regions, each with a single-parameter expert that acts as a constant predictor with zero-compute at inference. Motivated by high-rate quantization theory assumptions, we assume that the number of experts is sufficiently large to make their input-space regions very small. This lets us to study the approximation error of our MoE model class: (i) for one-dimensional inputs, we formulate the test error and its minimizing segmentation and experts; (ii) for multidimensional inputs, we formulate an upper bound for the test error and study its minimization. Moreover, we consider the learning of the expert parameters from a training dataset, given an input-space segmentation, and formulate their statistical learning properties. This leads us to theoretically and empirically show how the tradeoff between approximation and estimation errors in MoE learning depends on the number of experts.

Keywords: Mixture of experts, high-rate quantization theory, regression, approximation error, bias-complexity tradeoff.

1. Introduction

The mixture of experts (MoE) design for machine learning has been increasingly popular recently as a way to efficiently train large models on large datasets. The MoE design is usually implemented by routing inputs to one or more predictors, called experts, from an ensemble. Specifically, Sparse MoE (SMoE) designs ([Shazeer et al., 2017](#); [Riquelme et al., 2021](#); [Fedus et al., 2022b,a](#); [Liu et al., 2024](#)) adaptively choose (for a given input) a relatively small number of experts from the overall set of experts. This effectively reduces the data complexity that each expert should be responsible for its predictions; thus, each expert can be implemented by a simpler sub-model (e.g., less parameters, simpler functionality) that requires less training data. This leads to a more efficient training for the entire MoE model. While the recent trend is to use the MoE design for layer blocks within deep neural networks, the MoE was originally invented as a complete prediction model by itself.

The current popularity of MoE models calls for their foundational understanding. Indeed, recent MoE theories were provided by [Zhao et al. \(2024\)](#); [Jelassi et al. \(2025\)](#); [Nguyen et al. \(2023, 2024d,a,c,b\)](#); see Section 2.1 for an overview. Naturally, a comprehensive mathematical theory requires a relatively simple MoE; for example, the theory by [Jelassi et al. \(2025\)](#) is for a single-layer transformer model with 1-sparse MoE where a single expert is adaptively chosen for each input. Importantly, 1-sparse MoE designs are practically useful in deep learning ([Shazeer et al., 2017](#)).

In this paper, we provide a high-rate quantization theory perspective on 1-sparse MoE models for regression tasks. Our MoE includes many simple experts, specifically, the experts are learnable constant values that can provide predictions at inference without compute beyond routing the input to its expert. Accordingly, we call our design Zero-Compute 1-Sparse MoE (ZC-1SMoE). Despite

the per-expert simplicity, the use of many experts prevents over-simplicity from our ZC-1SMoE. Moreover, the idea of zero-compute experts was found by [Jin et al. \(2024\)](#) as practically useful for neural network MoEs; this further motivates our theory for ZC-1SMoE.

The use of many experts facilitates our use of famous high-rate quantization assumptions ([Bennett, 1948](#); [Panter and Dite, 1951](#); [Gersho, 1979](#); [Lloyd, 1982](#); [Na and Neuhoff, 1995](#); [Gray and Neuhoff, 1998](#)); see Section 2.2 and Appendix A. Our central assumption is that there are so many experts such that the input space is segmented to sufficiently small regions (each belongs to another expert) that allow to analytically approximate the discrete segmentation as a continuous density of segments. This plays a major role in our ZC-1SMoE analysis. Importantly, while we borrow ideas from high-rate quantization theory and its related use for piecewise-constant approximation of functions ([Dar and Bruckstein, 2019](#)), here we are the first to use these ideas for a *predictor learning* problem and its unique aspects that emerge from jointly handling both the input probability distribution and the input-to-output function (the latter function is due to the prediction problem and does not appear in standard quantization problems).

The main contributions of this paper stem from the novel use of high-rate quantization theory for the research of MoE learning, which provides new insights via the following:

1. Analysis of the approximation error of the ZC-1SMoE model class for one-dimensional inputs, including formulation of the test error and its minimizing segmentation and experts. Specifically, the optimal density of expert regions is formulated and shown how it can be used for forming the optimal one-dimensional input-space segmentation.
2. Analysis of the approximation error of the ZC-1SMoE model class for multidimensional inputs, including formulation of an upper bound for the test error and study of its minimization. The geometry of the expert regions is discussed and posed as a challenge for formulating the optimal multidimensional input-space segmentation.
3. Analysis of the learning of the expert parameters from a training dataset given an input-space segmentation, formulating their statistical learning properties. This includes theoretical and empirical analysis of the tradeoff between approximation and estimation errors in ZC-1SMoE learning and how it depends on the number of experts.

2. Relate Work

2.1. Theory for Mixture of Experts

[Zhao et al. \(2024\)](#) empirically and theoretically analyzed sparse MoE (SMoE) to elucidate how the sparsity level (the number of experts that are adaptively used from the overall set of experts) and task complexity (in terms of data distribution that combines more tasks/“skills”) affect the compositional generalization of the learned SMoE. Their theory analytically formulates the generalization error. Moreover, they heuristically define the big-O behavior of the approximation error and estimation error to explain a tradeoff as function of the sparsity level; by this, they explain that there is an optimal sparsity level that depends on the specific setting. Importantly, their approximation error does not depend on the overall number of experts, in contrast to the estimation error that we propose in this paper for the ZC-1SMoE. Moreover, our ZC-1SMoE setting lets us to propose a more analytically-justified decomposition of the test error to its approximation and estimation errors.

[Jelassi et al. \(2025\)](#) theoretically analyzed a single-layer transformer model with top-1 sparse MoE form. They show, also empirically on deep models, that increasing the overall number of experts is beneficial for memory-based tasks but not for reasoning tasks.

[Nguyen et al. \(2023, 2024d,a,c,b\)](#) theoretically studied the density and parameter estimation of MoE model for an unknown mixture data distribution using a Voronoi-cell loss definition. As the number of components (“experts”) in the true data distribution is unknown, the Voronoi cells assign the learned experts to their closest (unknown) true component (“expert”) of the data distribution. While Voronoi cells are related to quantization, the quantization perspective does not seem to appear in these works. Specifically, [Nguyen et al. \(2023, 2024d,a,c,b\)](#) significantly differ from this paper where we focus on the high-rate quantization theory (namely, segmentation of the input space to *many* regions) and consider a more general data distribution that rely on a non-mixture nonlinear unknown function plus noise.

MoE theories examine different learning approaches, for example, the maximum likelihood estimation is studied by [Nguyen et al. \(2023, 2024d,a\)](#), and learning via least squares is studied by [Nguyen et al. \(2024c,b\)](#). Here we also use the least squares learning approach and contribute to it the unique perspective of high-rate quantization theory.

2.2. High-Rate Quantization Theory

2.2.1. HIGH-RATE SCALAR QUANTIZATION THEORY

The high-rate quantization theory literature traces back to [Bennett \(1948\)](#) who provided an approximated error formula for nonuniform scalar quantization; remarkably, his error formula used integration over the continuous input domain, relaxing the discrete nature of the quantization cells. Namely, [Bennett \(1948\)](#) effectively assumed that the quantization cells are many and of sufficiently small sizes, such that the quantizer can be described by a smooth function (which also acts as an input compressor function that as a preprocessing can turn a uniform quantizer into a nonuniform quantizer; this is the compander design, which also requires a postprocessing function). This seminal work motivated a long line of research works on high-rate scalar quantization (see the comprehensive overview by [Gray and Neuhoff \(1998\)](#)). Notably, [Panter and Dite \(1951\)](#) used the integral error formula to characterize the optimal scalar quantizer based on the input probability distribution function. Moreover, [Lloyd \(1982\)](#) explicitly defined a differentiable density function of the quantizer cells over the continuous input domain; this density function generalizes the role of the derivative of the compressor function defined earlier by [Bennett \(1948\)](#). See Appendix A for formulations and more details.

2.2.2. HIGH-RATE VECTOR QUANTIZATION

The work by [Gersho \(1979\)](#) importantly extended the scope of high-rate quantization theory from scalar quantizers (that operate in one-dimensional space) to vector quantizers (that operate in multidimensional space). The principal challenge is that vector quantizers are based on input-space segmentation to multidimensional regions that have shapes and not just sizes (i.e., volumes); this contrasts the simpler case of scalar quantizers whose regions are “shapeless” intervals in the one-dimensional input domain. To analytically formulate the quantization error, [Gersho \(1979\)](#) introduced a conjecture on the shapes of the regions in optimal quantization (optimality in the sense of minimum mean squared error) for asymptotic input dimension – later on, this conjecture became famous and widely-believed ([Gray and Neuhoff, 1998](#)). According to the conjecture, for high-rate

(i.e., quantizer with many regions), most of the regions of an optimal d -dimensional vector quantizer are approximately congruent to a d -dimensional convex polytope that tessellates the d -dimensional space and is optimal in the sense of minimal normalized moment of inertia. Additional discussion on this conjecture is provided in Appendix B.

Another useful assumption given by [Na and Neuhoff \(1995\)](#) for high-rate vector quantization analysis is the existence of a smooth function (over the input space) that approximates the normalized moment of inertia of the segmentation regions. We use this assumption for bounding the approximation error of the MoE model class for the multidimensional inputs.

3. Problem and Model Definition

Consider a data model where the random input $\mathbf{x} \in [0, 1]^d$ is drawn from a probability distribution $P_{\mathbf{x}}$ over the d -dimensional unit cube, and the output y is a real value such that

$$y = \beta(\mathbf{x}) + \epsilon \quad (1)$$

where $\beta : [0, 1]^d \rightarrow \mathbb{R}$ is a non-random function unknown to the learner; $\epsilon \sim P_{\epsilon}$ is a real-valued random noise component with zero mean and variance σ_{ϵ}^2 . \mathbf{x} and ϵ are statistically independent.

The goal is to learn a mixture-of-experts predictor of the form

$$\hat{\beta}(\mathbf{x}) = c_i \text{ for } \mathbf{x} \in A_i \quad (2)$$

where the prediction for an input \mathbf{x} is determined based on a segmentation of the input space $[0, 1]^d$ into m regions $\{A_i\}_{i=1}^m$ that satisfy

$$\bigcup_{i=1}^m A_i = [0, 1]^d, \quad A_i \cap A_j = \emptyset \quad \forall i \neq j. \quad (3)$$

For any $i \in \{1, \dots, m\}$, the i^{th} region A_i is associated with a constant $c_i \in \mathbb{R}$. This MoE prediction model implies that a given input is routed to an expert based on the region that the input belongs to, and then the prediction is the region's constant without additional compute. Namely, each of the constants $\{c_i\}_{i=1}^m$ represents a zero-compute expert. We call this prediction model a zero-compute 1-sparse mixture of experts, which is abbreviated as ZC-1SMoE; in the rest of this paper, the term MoE refers to ZC-1SMoE, unless otherwise specified.

Let us denote the hypothesis class of the MoE for d -dimensional input as

$$\mathcal{H}_{m,d} = \left\{ \hat{\beta}(\mathbf{x}) = c_i \text{ for } \mathbf{x} \in A_i \mid \{c_i\}_{i=1}^m \in \mathbb{R}, \{A_i\}_{i=1}^m \text{ that satisfy (3)} \right\}. \quad (4)$$

Moreover, we define a simpler hypothesis class of MoE models for a *given* routing segmentation $\{A_i\}_{i=1}^m$ that satisfies (3):

$$\mathcal{H}_{m,d}^c(\{A_i\}_{i=1}^m) = \left\{ \hat{\beta}(\mathbf{x}) = c_i \text{ for } \mathbf{x} \in A_i \mid \{c_i\}_{i=1}^m \in \mathbb{R} \right\}, \quad (5)$$

namely, only the expert constants should be determined when learning/selecting a model from $\mathcal{H}_{m,d}^c(\{A_i\}_{i=1}^m)$.

The predictor form (2) motivates the following question:

- What is the best MoE predictor from the hypothesis class $\mathcal{H}_{m,d}$ (4) for a given data distribution $P_{\mathbf{x},y}$ that follows the data model (1)?

This question requires to answer two subsequent questions:

- What is the optimal input-space segmentation $\{A_i\}_{i=1}^m$ that defines the routing to experts?
- What are the optimal constants $\{c_i\}_{i=1}^m$ that define the experts predictions?

To answer these questions, we need to define a performance criterion – in our case this will be minimal prediction error on test data, which corresponds to the best generalization performance.

We consider a regression problem, the mean squared error (MSE) is used here to quantify prediction performance on a random input-output test pair (\mathbf{x}, y) drawn from the data model (1) independently of other draws (such as the training data, which will be studied later in Section 6). The test error of a predictor $\hat{\beta}$ is

$$\mathcal{E}_{\text{test}}(\hat{\beta}) = \mathbb{E}_{\mathbf{x}, y} \left[(\hat{\beta}(\mathbf{x}) - y)^2 \right]. \quad (6)$$

For the MoE model (2) with segmentation $\{A_i\}_{i=1}^m$ and expert constants $\{c_i\}_{i=1}^m$, the test error can be formulated (see Appendix D.1) as

$$\mathcal{E}_{\text{test}}(\{A_i\}_{i=1}^m, \{c_i\}_{i=1}^m) = \sigma_\epsilon^2 + \sum_{i=1}^m \int_{\mathbf{x} \in A_i} (c_i - \beta(\mathbf{x}))^2 p_{\mathbf{x}}(\mathbf{x}) d\mathbf{x}. \quad (7)$$

For a start, let us formulate the best predictor in the simpler hypothesis class $\mathcal{H}_{m,d}^c(\{A_i\}_{i=1}^m)$, which minimizes the test error

$$\hat{\beta}^{\text{opt}} = \arg \min_{\hat{\beta} \in \mathcal{H}_{m,d}^c(\{A_i\}_{i=1}^m)} \mathcal{E}_{\text{test}}(\hat{\beta}). \quad (8)$$

Solving this minimization problem (see Appendix D.2) yields that, for a given segmentation $\{A_i\}_{i=1}^m$, the optimal constants $\{c_i\}_{i=1}^m$ that minimize the test error are

$$c_i^{\text{opt}} = \frac{\int_{\mathbf{x} \in A_i} \beta(\mathbf{x}) p_{\mathbf{x}}(\mathbf{x}) d\mathbf{x}}{\int_{\mathbf{x} \in A_i} p_{\mathbf{x}}(\mathbf{x}) d\mathbf{x}}, \quad \forall i \in \{1, \dots, m\}. \quad (9)$$

The test error of the best predictor in a hypothesis class \mathcal{H} is known as the *approximation error* of \mathcal{H} (Shalev-Shwartz and Ben-David, 2014), a quantity that reflects the *inductive bias* of using \mathcal{H} for learning a predictor. Here, the approximation error of the MoE hypothesis class $\mathcal{H}_{m,d}^c(\{A_i\}_{i=1}^m)$ is

$$\mathcal{E}_{\text{app}}(\mathcal{H}_{m,d}^c(\{A_i\}_{i=1}^m)) = \min_{\hat{\beta} \in \mathcal{H}_{m,d}^c(\{A_i\}_{i=1}^m)} \mathcal{E}_{\text{test}}(\hat{\beta}). \quad (10)$$

The greater challenge is to formulate the best predictor in the hypothesis class $\mathcal{H}_{m,d}$, which minimizes the test error

$$\hat{\beta}^{\text{opt}} = \arg \min_{\hat{\beta} \in \mathcal{H}_{m,d}} \mathcal{E}_{\text{test}}(\hat{\beta}), \quad (11)$$

namely, to characterize the *jointly optimal* segmentation $\{A_i\}_{i=1}^m$ and expert constants $\{c_i\}_{i=1}^m$. Here, the approximation error of the MoE hypothesis class $\mathcal{H}_{m,d}$ is

$$\mathcal{E}_{\text{app}}(\mathcal{H}_{m,d}) = \min_{\hat{\beta} \in \mathcal{H}_{m,d}} \mathcal{E}_{\text{test}}(\hat{\beta}). \quad (12)$$

The formulation of the best in-class predictor and approximation error of $\mathcal{H}_{m,d}$ is the focus of Section 4 for one-dimensional inputs. The more intricate case of multidimensional inputs is addressed in Section 5 by formulating an upper bound to the approximation error and explaining the challenge in finding the optimal multidimensional segmentation. Section 6 analyzes the tradeoff between the approximation error and estimation error in learning MoE from $\mathcal{H}_{m,d}^c(\{A_i\}_{i=1}^m)$.

4. Approximation Error of MoE for One-Dimensional Inputs

In this section, we focus on the case of one-dimensional inputs that are drawn from a probability distribution P_x over the unit interval $[0, 1]$. Then, the data model (1) for $d = 1$ reduces to $y = \beta(x) + \epsilon$ where $\beta : [0, 1] \rightarrow \mathbb{R}$ is a non-random function unknown to the learner; $\epsilon \sim P_\epsilon$ is a real-valued random noise component with zero mean and variance σ_ϵ^2 . The formulations in Section 3 should be considered with $d = 1$ in this section. The notation of one-dimensional inputs and other scalar variables is not in bold font to emphasize differences from the multidimensional case.

Here, the regions $\{A_i\}_{i=1}^m$ that segment the input space are subintervals of the unit interval. Namely, $0 = a_0 < a_1 < \dots < a_{m-1} < a_m = 1$ are parameters that define m subintervals $A_i = [a_{i-1}, a_i]$, $i \in \{1, \dots, m\}$ that segment $[0, 1]$; formally, the m^{th} subinterval is $[a_{m-1}, a_m]$ but for writing simplicity it will be written as $[a_{m-1}, a_m]$ as the other subintervals. Accordingly, the multidimensional MoE from (2) reduces to the 1D-MoE model:

$$\hat{\beta}(x) = c_i \text{ for } x \in [a_{i-1}, a_i] \quad (13)$$

where $c_i \in \mathbb{R}$ is the constant expert of the i^{th} subinterval $[a_{i-1}, a_i]$.

For formulating the best predictor in the hypothesis class and its approximation error (i.e., solving (11), (12)), the important aspect of the 1D-MoE is that optimizing the input space segmentation is tractable, in contrast to the multidimensional case. This is because multidimensional regions $\{A_i\}_{i=1}^m$ are defined by their volumes and shapes. In contrast, segmenting the unit interval requires to optimize $m - 1$ scalar variables $\{a_i\}_{i=1}^{m-1}$ that create subintervals by determining their lengths (which take the role of region volumes) without any other optimizable aspect of shape.

For the 1D-MoE from (13) with segmentation parameters $\{a_i\}_{i=0}^m$ and expert constants $\{c_i\}_{i=1}^m$, the test error (7) becomes

$$\mathcal{E}_{\text{test}}(\{a_i\}_{i=0}^m, \{c_i\}_{i=1}^m) = \sigma_\epsilon^2 + \sum_{i=1}^m \int_{x=a_{i-1}}^{a_i} (c_i - \beta(x))^2 p_x(x) dx. \quad (14)$$

From (9) we get that the optimal expert constant for a given subinterval $[a_{i-1}, a_i]$ is

$$c_i^{\text{opt}} = \frac{\int_{x=a_{i-1}}^{a_i} \beta(x) p_x(x) dx}{\int_{x=a_{i-1}}^{a_i} p_x(x) dx}. \quad (15)$$

4.1. Small Subintervals Assumption and Locally-Linear Approximations

We now assume that there are many experts (i.e., m is high) such that the subintervals are small and, therefore, allow locally-linear approximations of β and p_x . For the i^{th} subinterval, we denote its

length as $\Delta_i \triangleq a_i - a_{i-1}$ and its center as $x_i \triangleq \frac{a_{i-1} + a_i}{2}$. Then, the first-order Taylor approximation of β around the i^{th} subinterval center x_i is

$$\beta(x) = \beta(x_i) + \beta'(x_i) \cdot (x - x_i) + R_{\beta,1}(x) \quad (16)$$

where $R_{\beta,1} \in o(|x - x_i|)$ is a remainder term. Similarly, the approximation for the probability density function of x is

$$p_x(x) = p_x(x_i) + p'_x(x_i) \cdot (x - x_i) + R_{p_x,1}(x) \quad (17)$$

where $R_{p_x,1} \in o(|x - x_i|)$ is a remainder term. Using the locally-linear approximations (16)-(17), the optimal expert constants (15) and test error (14) can be formulated as follows.

Theorem 1 *Given a segmentation of $[0, 1]$ by m subintervals $\{[a_{i-1}, a_i]\}_{i=1}^m$, the optimal expert constants are*

$$c_i^{\text{opt}} = \beta(x_i) + o(\Delta_i) \text{ as } \Delta_i \rightarrow 0, \quad \forall i \in \{1, \dots, m\}. \quad (18)$$

The corresponding test error can be formulated as

$$\mathcal{E}_{\text{test}} = \sigma_\epsilon^2 + \frac{1}{12} \sum_{i=1}^m (\beta'(x_i))^2 p_x(x_i) \Delta_i^3 + o(\Delta_{\max}^3) \quad (19)$$

where $\Delta_{\max} = \max_{i \in \{1, \dots, m\}} \Delta_i$ is the largest subinterval length.

The proof is in Appendix E.1. The test error in (19) is the approximation error \mathcal{E}_{app} of the hypothesis class $\mathcal{H}_{m,1}^c(\{[a_{i-1}, a_i]\}_{i=1}^m)$; recall the definitions in (5), (10).

4.2. Optimizing the Routing Segmentation using Expert Segment Density

Motivated by the density function of quantization cells in high-rate quantization theory (defined for scalar quantization by Lloyd (1982) and for vector quantization by Gersho (1979); Na and Neuhoff (1995)), we now define a density function for the input-space segments of experts in our problem.

Assumption 1 *There exists an expert segment density function $\lambda : [0, 1] \rightarrow \mathbb{R}_+$ which is smooth and satisfies*

$$\lambda(x) \approx \frac{1}{m\Delta_i} \text{ for } x \in [a_{i-1}, a_i]. \quad (20)$$

Therefore, at the subinterval centers, $\lambda(x_i) \approx \frac{1}{m\Delta_i}$, $\Delta_i \approx \frac{1}{m\lambda(x_i)}$, $\forall i \in \{1, \dots, m\}$.

Using Assumption 1 and approximating the sum in (19) as integral due to the small segment assumption, we get the following test error formula as a corollary of Theorem 1.

Corollary 2 *The test error for optimal expert constants can be approximated using continuous integration: $\mathcal{E}_{\text{test}} \approx \tilde{\mathcal{E}}_{\text{test}}$ where*

$$\tilde{\mathcal{E}}_{\text{test}} = \sigma_\epsilon^2 + \frac{1}{12m^2} \int_{x=0}^1 \frac{(\beta'(x))^2 p_x(x)}{\lambda^2(x)} dx. \quad (21)$$

In high-rate quantization theory, related integral formulas of the error (e.g., (45) in Appendix A.1) were informally justified based on the large number of segments (quantization cells) by [Bennett \(1948\)](#); [Panter and Dite \(1951\)](#); [Lloyd \(1982\)](#), and formally justified by [Na and Neuhoff \(1995\)](#) for vector quantizers using a series of quantizers whose number of segments goes to infinity. A formal proof of (21) is omitted here, as it is technically similar to the proof by [Na and Neuhoff \(1995\)](#). More details on (21) are provided in Appendix E.2.

Using the error formula from (21), the following theorem provides the optimal expert segment density function λ^{opt} and its corresponding optimal error.

Theorem 3 *The test error $\tilde{\mathcal{E}}_{\text{test}}$ (21) is minimized by the optimal expert segment density function*

$$\lambda^{\text{opt}}(x) = \frac{\sqrt[3]{p_x(x) (\beta'(x))^2 dx}}{\int_{\xi=0}^1 \sqrt[3]{p_x(\xi) (\beta'(\xi))^2 d\xi}} \quad (22)$$

that attains the minimal test error of

$$\tilde{\mathcal{E}}_{\text{test}}^{\text{opt}} = \sigma_{\epsilon}^2 + \frac{1}{12m^2} \left(\int_{x=0}^1 \sqrt[3]{p_x(x) (\beta'(x))^2 dx} \right)^3. \quad (23)$$

The theorem proof is provided in Appendix E.3. The test error in (23) corresponds to the approximation error \mathcal{E}_{app} of the hypothesis class $\mathcal{H}_{m,1}$; recall the definitions in (4), (12).

In Section 4.4 we provide and discuss the empirical evaluations that correspond to the theory in this section; showcasing the optimal segmentations, expert constants, segment density functions, and that the approximation error formula (23) excellently matches the empirical evaluation on test data (unless the number of experts is too small, as reasonable due to our many-experts assumption).

4.3. Differences Between the 1D-MoE Learning and Scalar Quantization

Let us highlight some of the prominent differences between our current analysis and the classical high-rate quantization analysis. Many differences between the two tasks emerge from their basic error formulations that should be minimized; i.e., see that the MoE test error (14) involves both p_x and β , whereas the quantization error (42) is based only on p_x and there is no β in the problem — this important difference holds even before the high-rate assumptions. Then, for MoE learning we assume local linearity for p_x (17) and β (16); in contrast, for scalar quantization, p_x is assumed as locally constant (43) and there is no β in the problem. Moreover, the optimal expert constants (18) are approximately the β evaluations at the interval midpoints, whereas the optimal quantizer representations are just the interval midpoints (44).

Importantly, for MoE learning, the error and its minimizing segment density and value depend on the product between the the input PDF p_x and the squared derivative of the input-output relation function $(\beta'(x))^2$; whereas for scalar quantization the dependency is only on the input PDF p_x . To observe this, compare (21), (22), (23) with (45), (46), (47), respectively.

4.4. Empirical Results: Approximation Error, Optimal Segmentation and Experts

In Figs. 1-2 we empirically exemplify the optimal segmentation that corresponds to the optimal segment density λ^{opt} from Eq. (22) of Theorem 3. The discrete segmentation is formed by the

formulations (49)-(50) of Appendix A.2 but instead of the quantizer density g^{opt} we use our MoE density λ^{opt} from (22).

Recall that (49) has a unique solution for a density which is positive over $[0, 1]$. However, even if we assume $p_x(x) > 0, \forall x \in [0, 1]$, our density λ^{opt} may have zero values for $x \in [0, 1]$ such that $\beta'(x) = 0$. As explained by [Dar and Bruckstein \(2019\)](#) for piecewise-constant approximation of a given function (without learning), the empirical difficulty is when β is constant (and therefore $\beta'(x) = 0$) over a continuous sub-interval of the input domain. They also showed that this can be empirically addressed by replacing the zero-derivative values with an arbitrarily-small constant. Accordingly, we empirically compute λ^{opt} from (22) with replacing the near zero values $p_x(x) (\beta'(x))^2 < \text{eps}$ with eps where the numerical precision value eps is in the order of 10^{-16} . In Fig. 2 we show results for a setting that significantly needs this mechanism.

The experiments settings of Figs. 1-2 differ only in the true β function. In Fig. 1, $\beta(x) = \cos(10\pi x)$ for $x \in [0, 1]$. In Fig. 2, $\beta(x) = \cos(10\pi x)$ for $x \in [0, 0.4] \cup [0.6, 1]$ and $\beta(x) = 1$ for $x \in (0.4, 0.6)$. The β function is used in the one-dimensional data model $y = \beta(x) + \epsilon$ from Section 4; here, the noise ϵ is a uniform random variable from the continuous range $[-0.1, 0.1]$. Both experiments demonstrate that the optimal segment density is higher for inputs whose product of the input probability density function p_x and the squared derivative of β is relatively high; see Figs. 1(d) and 2(d), which empirically compute λ^{opt} that was provided in Eq. (22) of Theorem 3.

Figs. 1(e)-1(g), 2(e)-2(g) show the best predictors in the MoE hypothesis class $\mathcal{H}_{m,1}$, where both the segmentation and the expert constant are model parameters, as defined in (4); the magenta lines show the best in-class predictor, β^{opt} from (11). The red markers on the x -axis show the points $\{a_i\}_{i=1}^m$ of the optimal segmentation that was formed from the optimal density λ^{opt} . It can be observed that relatively smaller segments are assigned for when λ^{opt} is higher (due to a relatively higher product of the input probability density function p_x and the squared derivative of β).

Figs. 1(h), 2(h) show the approximation error curves for a varying number of experts m . The empirical curve, in solid blue line, was computed as the average squared error of the best-in class predictor (for each m) for a dataset of 5000 test examples (note that here, in the approximation error evaluation, there is no learning from training dataset). The theoretical curve, in dotted red line, was numerically computed by (23) of Theorem 3. The evaluations show excellent match between the empirical evaluation and the theoretical formula; significant differences between the two are observed in Fig. 1(h) for a small number of experts ($m < 14$) but this is reasonable considering the theoretical assumption of having many experts (i.e., sufficiently large m).

5. Approximation Error of MoE for Multidimensional Inputs

We now return to the general case of multidimensional inputs, as presented in Section 3. While some of the detailed analysis naturally extend the one-dimensional case of Section 4, the multidimensional case has important differences that affect the test error formulation and segmentation optimization.

Each region has a volume $V(A_i) \triangleq \int_{\mathbf{x} \in A_i} d\mathbf{x}$, center $\mathbf{x}_i \triangleq \int_{\mathbf{x} \in A_i} \mathbf{x} d\mathbf{x}$, and shape that is reflected by the normalized second-moment of inertia about the center \mathbf{x}_i :

$$M(A_i) \triangleq \frac{\int_{\mathbf{x} \in A_i} \|\mathbf{x} - \mathbf{x}_i\|_2^2 d\mathbf{x}}{d \cdot V(A_i)^{1+\frac{2}{d}}} \quad (24)$$

where the normalization makes $M(A_i)$ invariant to proportional scaling of a given shape of A_i .

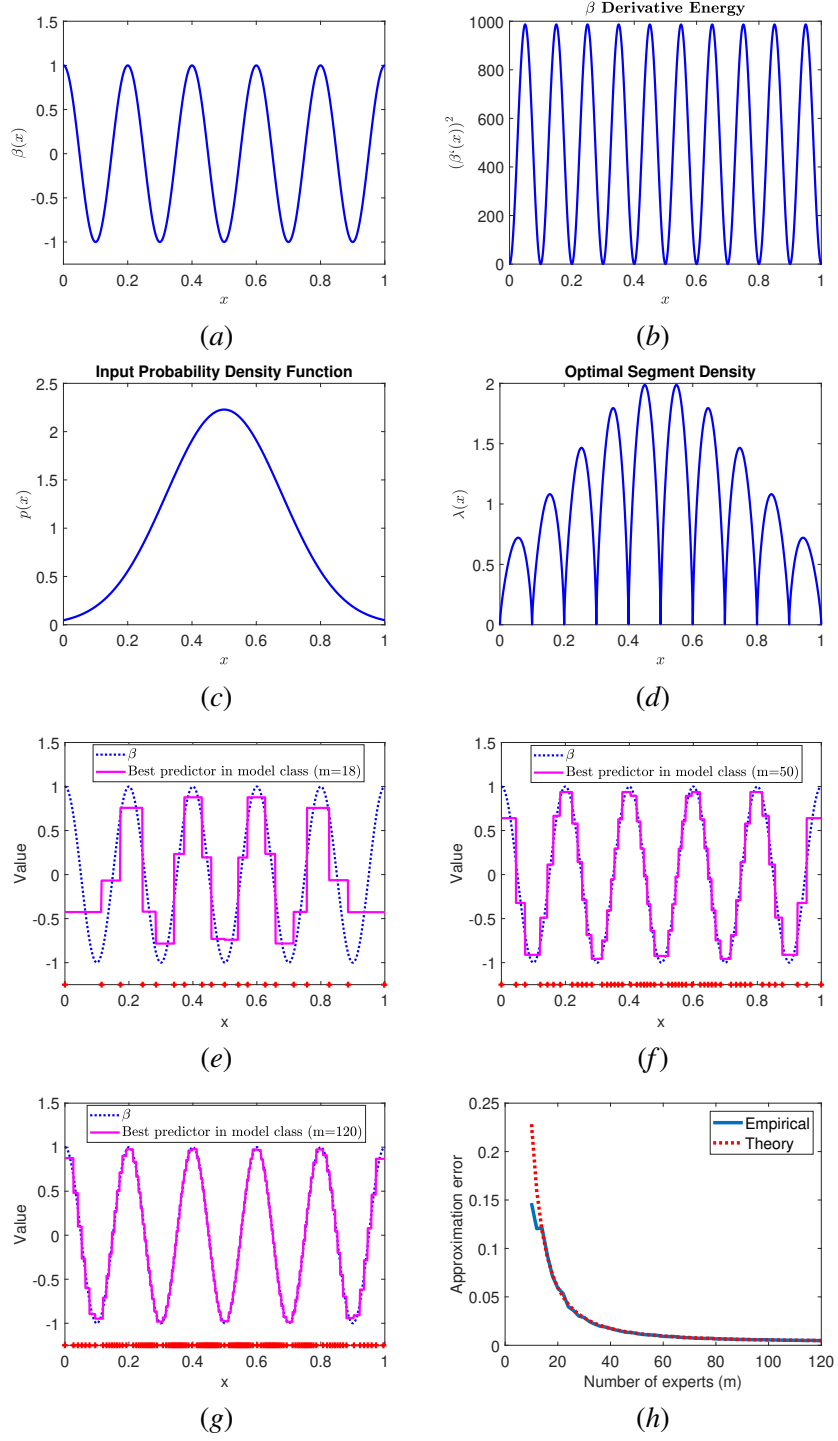


Figure 1: Examples for optimal segmentation, best predictor in $\mathcal{H}_{m,1}$, and approximation error curves for a **cosine** β and truncated Gaussian p_x . In (e)-(g), the red markers on the x -axis denote the optimal segmentation points $\{a_i\}_{i=1}^m$ that were formed from the optimal segment density in (d).

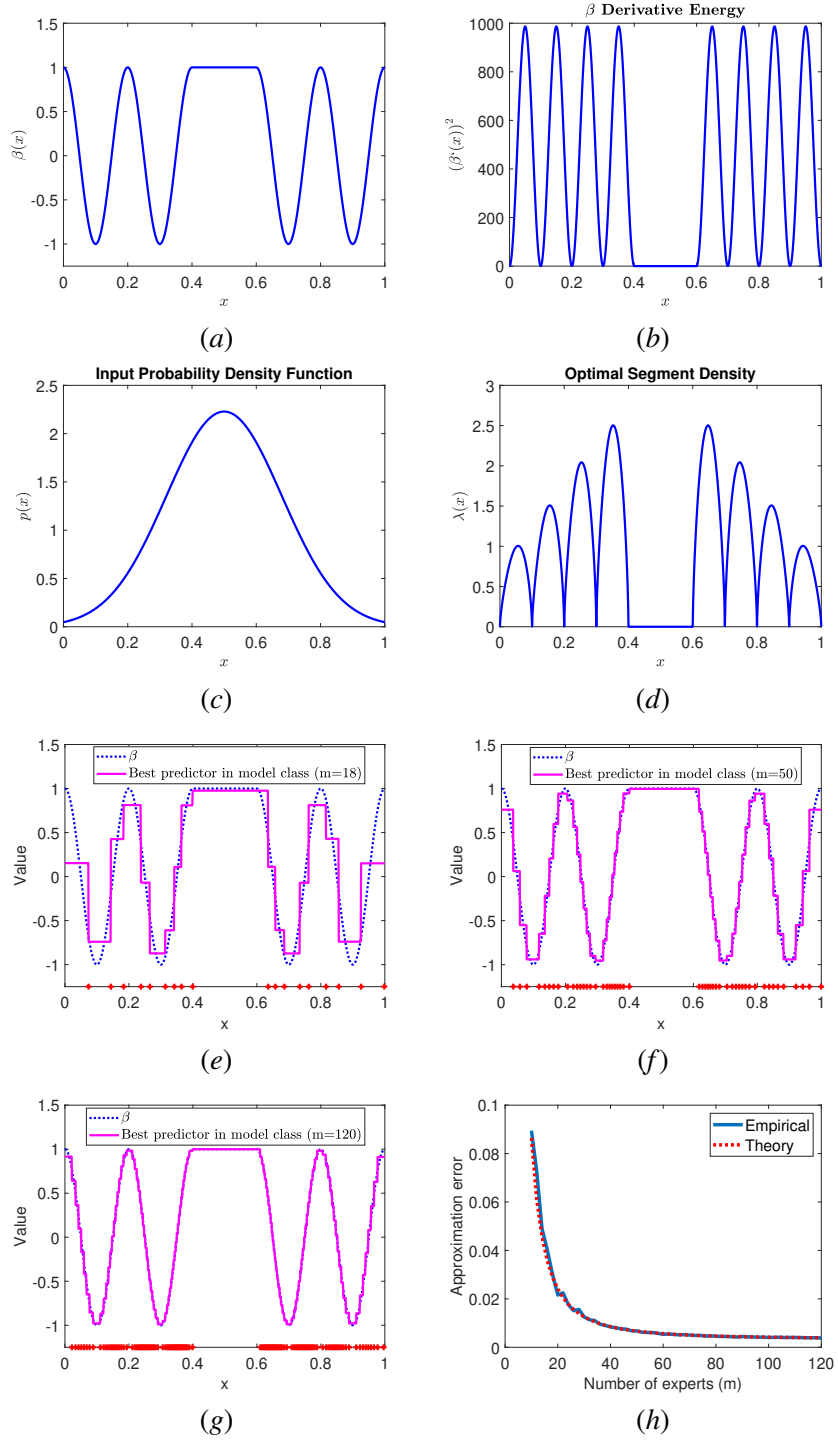


Figure 2: Examples for optimal segmentation, best predictor in $\mathcal{H}_{m,1}$, and approximation error curves for a **cosine with a constant segment** β and truncated Gaussian p_x . In (e)-(g), the red markers on the x -axis denote the optimal segmentation points $\{a_i\}_{i=1}^m$ that were formed from the optimal segment density in (d).

We assume that there are many experts such that their d -dimensional regions $\{A_i\}_{i=1}^m$ are sufficiently small to allow locally-linear approximations of β and $p_{\mathbf{x}}$. Specifically, the first-order Taylor approximations of β and $p_{\mathbf{x}}$ around the i^{th} region center \mathbf{x}_i are

$$\beta(\mathbf{x}) = \beta(\mathbf{x}_i) + \nabla\beta(\mathbf{x}_i)^T(\mathbf{x} - \mathbf{x}_i) + R_{\beta,1}(\mathbf{x}) \quad (25)$$

$$p_{\mathbf{x}}(\mathbf{x}) = p_{\mathbf{x}}(\mathbf{x}_i) + \nabla p_{\mathbf{x}}(\mathbf{x}_i)^T(\mathbf{x} - \mathbf{x}_i) + R_{p_{\mathbf{x}},1}(\mathbf{x}) \quad (26)$$

where $\nabla\beta(\mathbf{x}_i)$ and $\nabla p_{\mathbf{x}}(\mathbf{x}_i)$ are the gradients of β and $p_{\mathbf{x}}$, respectively, at the region center \mathbf{x}_i ; $R_{\beta,1} \in o(\|\mathbf{x} - \mathbf{x}_i\|_2)$ and $R_{p_{\mathbf{x}},1} \in o(\|\mathbf{x} - \mathbf{x}_i\|_2)$ are remainder terms.

Using the locally-linear approximations (25)-(26), the optimal expert constants (9) can be formulated and their test error (7) can be upper bounded as follows (see proof in Appendix F.1).

Theorem 4 *For a given segmentation of $[0, 1]^d$ by m regions $\{A_i\}_{i=1}^m$, the optimal expert constants are*

$$c_i^{\text{opt}} = \beta(\mathbf{x}_i) + o\left(V(A_i)^{1/d}\right) \text{ as } V(A_i) \rightarrow 0, \quad \forall i \in \{1, \dots, m\}. \quad (27)$$

The corresponding test error can be upper bounded as

$$\mathcal{E}_{\text{test}}\left(\{A_i\}_{i=1}^m, \{c_i^{\text{opt}}\}_{i=1}^m\right) \leq \sigma_{\epsilon}^2 + d \sum_{i=1}^m \|\nabla\beta(\mathbf{x}_i)\|_2^2 p_{\mathbf{x}}(\mathbf{x}_i) M(A_i) V(A_i)^{1+\frac{2}{d}} + o\left(V_{\max}^{1+\frac{2}{d}}\right) \quad (28)$$

where $M(A_i)$ is the normalized second-moment of inertia of A_i , and $V_{\max} = \max_{i \in \{1, \dots, m\}} V(A_i)$ is the largest region volume.

The test error on the left side in (28) is the approximation error \mathcal{E}_{app} of the hypothesis class $\mathcal{H}_{m,d}^c(\{A_i\}_{i=1}^m)$; this is due to the definitions in (5), (10) and the proof of (28) where the optimal constants are set in the test error formula *before* developing the upper bound. Importantly, note that (28) is an upper bound on the test error and not formulation with equality as in the one-dimensional input case (19); this is due to the Cauchy-Schwarz inequality applications on the inner products of gradients and centered input vectors, for more details see (99)-(101) in the proof (Appendix F.1).

Motivated by high-rate vector quantization theory (Gersho, 1979; Na and Neuhoff, 1995), we define a density function for the input-space segments of experts in our multidimensional problem (extending Assumption 1 for one-dimensional inputs).

Assumption 2 *There exists an expert segment density function $\lambda : [0, 1]^d \rightarrow \mathbb{R}_+$ which is smooth and satisfies $\lambda(\mathbf{x}) \approx \frac{1}{mV(A_i)}$ for $\mathbf{x} \in A_i$. Therefore, at the region centers, $\lambda(\mathbf{x}_i) \approx \frac{1}{mV(A_i)}$, $V(A_i) \approx \frac{1}{m\lambda(\mathbf{x}_i)}$, $\forall i \in \{1, \dots, m\}$.*

The multidimensional case requires to consider the segmentation region shapes, and specifically their normalized moment of inertia $\{M(A_i)\}_{i=1}^m$ that appear in (28). Similarly to the vector quantization analysis by Na and Neuhoff (1995), the following assumption will be analytically useful.

Assumption 3 *There exists a smooth function $\mu : [0, 1]^d \rightarrow \mathbb{R}_+$, known as the normalized moment of inertia profile, that satisfies*

$$\mu(\mathbf{x}) \approx M(A_i) \text{ for } \mathbf{x} \in A_i. \quad (29)$$

Therefore, at the region centers, $\mu(\mathbf{x}_i) \approx M(A_i)$, $\forall i \in \{1, \dots, m\}$.

Using Assumptions 2-3 and approximating the sum in (28) as integral due to the small segment assumption, we get an approximated formula for the error upper-bound as corollary of Theorem 4.

Corollary 5 *The upper bound on the test error for optimal constants can be approximated using continuous integration: $\mathcal{E}_{\text{test}} \leq \mathcal{E}_{\text{test}}^{\text{bound}} \approx \tilde{\mathcal{E}}_{\text{test}}^{\text{bound}}$ where*

$$\tilde{\mathcal{E}}_{\text{test}}^{\text{bound}} = \sigma_{\epsilon}^2 + \frac{d}{m^{2/d}} \int_{\mathbf{x} \in [0,1]^d} \frac{\|\nabla \beta(\mathbf{x})\|_2^2 p_{\mathbf{x}}(\mathbf{x}) \mu(\mathbf{x})}{\lambda^{2/d}(\mathbf{x})} d\mathbf{x} \quad (30)$$

where $\mu(\mathbf{x})$ is a smooth moment of inertia profile from Assumption 3.

More details on (30) are provided in Appendix F.2.

Recall that the volume of the d -dimensional unit cube is 1, therefore cases where the value of $\frac{\|\nabla \beta(\mathbf{x})\|_2^2 p_{\mathbf{x}}(\mathbf{x}) \mu(\mathbf{x})}{\lambda^{2/d}(\mathbf{x})}$ for $\mathbf{x} \in [0,1]^d$ can be upper bounded by a constant agnostic of m and d motivate the following assumption.

Assumption 4 $\int_{\mathbf{x} \in [0,1]^d} \frac{\|\nabla \beta(\mathbf{x})\|_2^2 p_{\mathbf{x}}(\mathbf{x}) \mu(\mathbf{x})}{\lambda^{2/d}(\mathbf{x})} d\mathbf{x}$ can be upper bounded by a constant agnostic of m and d .

Then, Corollary 5 implies the following big-O bound on the approximation error.

Corollary 6 *Under Assumption 4, the approximation error satisfies*

$$\mathcal{E}_{\text{app}}(\mathcal{H}_{m,d}^c(\{A_i\}_{i=1}^m)) = \sigma_{\epsilon}^2 + \mathcal{O}\left(\frac{d}{m^{2/d}}\right) \quad (31)$$

where $\{A_i\}_{i=1}^m$ is a discrete segmentation that theoretically corresponds to a given segment density $\lambda(\mathbf{x})$ for all m .

In Appendix C, we continue to analyze the minimization of the upper bound by the segmentation — although the bound of Corollary 6 is sufficient for analyzing the statistical learning with $\mathcal{H}_{m,d}^c(\{A_i\}_{i=1}^m)$ in the next section.

6. Learning the Constant Experts: A Tradeoff in the Number of Experts

The previous sections studied the approximation error of the MoE model classes (4) and (5), namely, the best performance that these model classes can achieve for a given data distribution (i.e., known input and noise distributions and the true β that defines the output distribution). Now, we turn to study the generalization aspect of learning the expert constants from training examples (and without knowing the true data distribution) for our MoE model with a given routing segmentation of the input space.

6.1. Learning Expert Constants via Least Squares

Consider a training dataset of n input-output examples $\mathcal{S}_n \triangleq \{(\mathbf{x}^{(j)}, y^{(j)})\}_{j=1}^n$ i.i.d. drawn from the data model (1). The j^{th} training example satisfies the data model

$$y^{(j)} = \beta(\mathbf{x}^{(j)}) + \epsilon^{(j)} \quad (32)$$

where $\epsilon^{(j)}$ is the underlying noise component.

Importantly, now we do not know the true β nor the input PDF $p_{\mathbf{x}}$, therefore computation of the optimal expert constants directly via (9) or (27) is impossible. Instead, we learn the expert constants for a given routing segmentation $\{A_i\}_{i=1}^m$. This corresponds to learning a model from the hypothesis class $\mathcal{H}_{m,d}^c(\{A_i\}_{i=1}^m)$, as defined in (5).

We define $q_i^{(j)}$ as an indicator for the inclusion of the j^{th} training input $\mathbf{x}^{(j)}$ in the i^{th} region A_i ,

$$q_i^{(j)} \triangleq \mathbb{I} \left[\mathbf{x}^{(j)} \in A_i \right] \quad (33)$$

where $\mathbb{I}[\text{condition}]$ returns 1 if its condition is satisfied, and 0 otherwise. Accordingly, the number of training examples that are routed to the i^{th} expert is

$$n_i \triangleq \sum_{j=1}^n q_i^{(j)}. \quad (34)$$

Then, for a given routing segmentation $\{A_i\}_{i=1}^m$, the i^{th} expert constant is learned via least squares

$$\forall i \in \{1, \dots, m\} \text{ such that } n_i > 0, \quad \tilde{c}_i = \arg \min_{v \in \mathbb{R}} \sum_{j: q_i^{(j)}=1} \left(v - y^{(j)} \right)^2 = \frac{1}{n_i} \sum_{j: q_i^{(j)}=1} y^{(j)}. \quad (35)$$

Note that the i^{th} expert constant is learned only from the examples that are routed to it. As we consider here a fixed, non-learned input-space segmentation, there is some probability that a region might not get training examples (i.e., $n_i = 0$ for some i); in such regions, one may apply a globally default value for the expert, for example, if $n_i = 0$ set the average of all outputs in the training dataset $\tilde{c}_i = \frac{1}{n} \sum_{j=1}^n y^{(j)}$. This will be useful for the empirical analysis in Appendix 6.3. The theoretical analysis below will focus on the main case of (35).

The following theorem shows that the learned expert constant \tilde{c}_i for unknown β (and $n_i > 0$) is an unbiased estimate of the optimal expert constant c_i^{opt} for known β . The proof is in Appendix G.1

Theorem 7 *The expectation of the expert constant \tilde{c}_i learned via (35) given $n_i > 0$ training examples is the optimal expert constant c_i^{opt} : $\mathbb{E}[\tilde{c}_i | n_i > 0] = c_i^{\text{opt}}$.*

6.2. Test Error Analysis for MoE with Learned Expert Constants

We start the analysis by decomposing the test error of the MoE with learned constants. The probability of the input routed to the i^{th} expert is denoted as

$$\rho_i \triangleq \text{Prob} [\mathbf{x} \in A_i]. \quad (36)$$

Lemma 8 *For a given routing segmentation $\{A_i\}_{i=1}^m$, the test error of MoE with learned constants $\{\tilde{c}_i\}_{i=1}^m$ can be decomposed as*

$$\mathcal{E}_{\text{test}}(\{A_i\}_{i=1}^m, \{\tilde{c}_i\}_{i=1}^m) = \mathcal{E}_{\text{app}}(\mathcal{H}_{m,d}^c(\{A_i\}_{i=1}^m)) + \mathcal{E}_{\text{est}}(m, \mathcal{S}_n) \quad (37)$$

where the approximation error equals the test error of MoE with optimal constants $\{c_i^{\text{opt}}\}_{i=1}^m$, i.e.,

$$\mathcal{E}_{\text{app}}(\mathcal{H}_{m,d}^c(\{A_i\}_{i=1}^m)) = \mathcal{E}_{\text{test}}\left(\{A_i\}_{i=1}^m, \{c_i^{\text{opt}}\}_{i=1}^m\right), \quad (38)$$

and the estimation error, which reflects the statistical learning of m expert constants from the training dataset \mathcal{S}_n , is formulated as

$$\mathcal{E}_{\text{est}}(m, \mathcal{S}_n) = \sum_{i=1}^m (\tilde{c}_i - c_i^{\text{opt}})^2 \rho_i. \quad (39)$$

See proof in Appendix G.2. This theorem decomposes the MoE test error into approximation error and estimation error, a decomposition which is widely used in machine learning theory (see, e.g., (Shalev-Shwartz and Ben-David, 2014)).

The test error expression in Lemma 8 motivates us to analyze the statistical behavior of the distance $|\tilde{c}_i - c_i^{\text{opt}}|$ between the learned constants and their optimal counterparts. First, let us formulate concentration bounds for the number n_i of training examples that are routed to the i^{th} expert.

Lemma 9 For $\tilde{\delta} \in (0, 1)$ and given $n \geq \frac{8}{\rho_i} \ln\left(\frac{1}{\tilde{\delta}}\right)$,

$$\text{Prob}\left[n_i > \frac{1}{2}n\rho_i\right] \geq 1 - \tilde{\delta}.$$

The proof uses the Chernoff bound for a sum of independent Bernoulli variables; see Appendix G.3.

Then, using Lemma 9 and assuming the noise ϵ in the data model (1) is from a bounded range, the distance $|\tilde{c}_i - c_i^{\text{opt}}|$ is statistically bounded as follows.

Theorem 10 Consider the i^{th} region A_i , whose value range size of β is denoted as $R_{\beta,i} \triangleq \max_{\mathbf{x} \in A_i} \beta(\mathbf{x}) - \min_{\mathbf{x} \in A_i} \beta(\mathbf{x})$. Assume a positive probability $\rho_i > 0$ for the input routed to A_i . Assume the noise ϵ is from the bounded range $[\epsilon_{\min}, \epsilon_{\max}]$ and denote $R_\epsilon \triangleq \epsilon_{\max} - \epsilon_{\min}$. Then, for $\gamma \geq 0$, $\tilde{\delta} \in (0, 1)$, and given $n \geq \frac{8}{\rho_i} \ln\left(\frac{1}{\tilde{\delta}}\right)$,

$$|\tilde{c}_i - c_i^{\text{opt}}| < \gamma \frac{R_{\beta,i} + R_\epsilon}{\sqrt{n\rho_i}} \quad (40)$$

with probability at least $1 - 2 \exp(-\gamma^2) - \tilde{\delta}$.

The proof is provided in Appendix G.4.

Next, using Lemma 8 and Theorem 10, the test error of MoE with learned constants $\{\tilde{c}_i\}_{i=1}^m$ can be upper bounded as follows (proof in Appendix G.5).

Theorem 11 For a given routing segmentation $\{A_i\}_{i=1}^m$ with $\rho_i > 0 \ \forall i$, $\gamma \geq 0$, $\tilde{\delta} \in (0, 1)$, and given $n \geq \frac{8}{\min_{i \in \{1, \dots, m\}} \rho_i} \ln\left(\frac{1}{\tilde{\delta}}\right)$,

$$\mathcal{E}_{\text{est}}(m, \mathcal{S}_n) < \frac{m}{n} \gamma^2 \max_{i \in \{1, \dots, m\}} (R_{\beta,i} + R_\epsilon)^2 \quad (41)$$

with probability at least $1 - 2m \exp(-\gamma^2) - m\tilde{\delta}$.

The upper bound on the estimation error in Theorem 11 implies $\mathcal{E}_{\text{est}}(m, \mathcal{S}_n) \in \mathcal{O}\left(\frac{m}{n}\right)$. By Corollary 6, we already know that the approximation error behaves as $\mathcal{E}_{\text{app}}\left(\mathcal{H}_{m,d}^c(\{A_i\}_{i=1}^m)\right) = \sigma_\epsilon^2 + \mathcal{O}\left(\frac{d}{m^{2/d}}\right)$. Therefore, by the test error decomposition (37), there is a tradeoff in the test error as function of the number of experts m . Considering a fixed input dimension d and a fixed dataset size n , the tradeoff is based on two contradicting trends: For MoE with more experts, i.e., increasing m ,

- the MoE expressiveness improves as reflected by reduction in the approximation error as $\mathcal{O}\left(\frac{d}{m^{2/d}}\right)$;
- the statistical learning degrades, as each expert is trained on less examples out of the n training examples, leading to estimation error that increases as $\mathcal{O}\left(\frac{m}{n}\right)$.

This theoretical tradeoff is qualitatively supported by our empirical results for one-dimensional inputs in the following subsection.

6.3. Empirical Results: Learning Experts from Training Data for MoE with Uniform Segmentation for One-Dimensional Inputs

Now we proceed to experiments of learning the constant experts from a given training dataset. Similarly to Section 6, the considered MoE is for a given segmentation (which is not necessarily optimal) that does not need to be learned; here the segmentation will be uniform, i.e., $a_i = \frac{i}{m}$ for $i \in \{1, \dots, m\}$ for the one-dimensional MoE class $\mathcal{H}_{m,1}^c(\{a_i = \frac{i}{m}\}_{i=1}^m)$, as was more generally defined in (5).

The learning of the expert constants is by the region-based least squares solution in (35), and with the exception that expert constants of regions without training examples are set as the average of all outputs in the training dataset. The learning experiment results are provided in Figs. 3-4. Figs. 3(a)-3(b), 4(a)-4(b) show the differences between the learned constants (in the learned predictors, shown as solid black lines) and the optimal constants (in the best in-class nonlearned predictors, computed by (15) for the uniform segmentation, and shown as dotted magenta lines).

Figs. 3(c), 4(c) show the approximation error curves for the model class $\mathcal{H}_{m,1}^c(\{a_i = \frac{i}{m}\}_{i=1}^m)$. There is an excellent match between the empirical evaluation (on a test dataset of 5000 examples) and the numerical evaluation of the theoretical error formula from (21) that is suitable also for suboptimal segment densities, as we have here with the uniform segmentation.

Figs. 3(d), 4(d) show the test error curves for three different sizes of training dataset. These test error values were computed empirically as the average over 300 experiments, each with another randomly drawn training dataset. The test error curves qualitatively demonstrate the tradeoff between the approximation error and the estimation error as function of the number of experts m , as discussed in Section 6.2. Specifically, the test error curve first decreases with m , due to the significant decrease of the approximation error that dominates the overall test error trend for sufficiently small m ; then, the test error curve increases with m , due to the increase of the estimation error that dominates the overall test error trend for sufficiently large m . It can be observed that the minimal test error is obtained for a larger m if the training dataset is larger; this is because having more training data increases the probability of having more training examples in each region, which in return allows the regions to be smaller without increasing the estimation error too much.

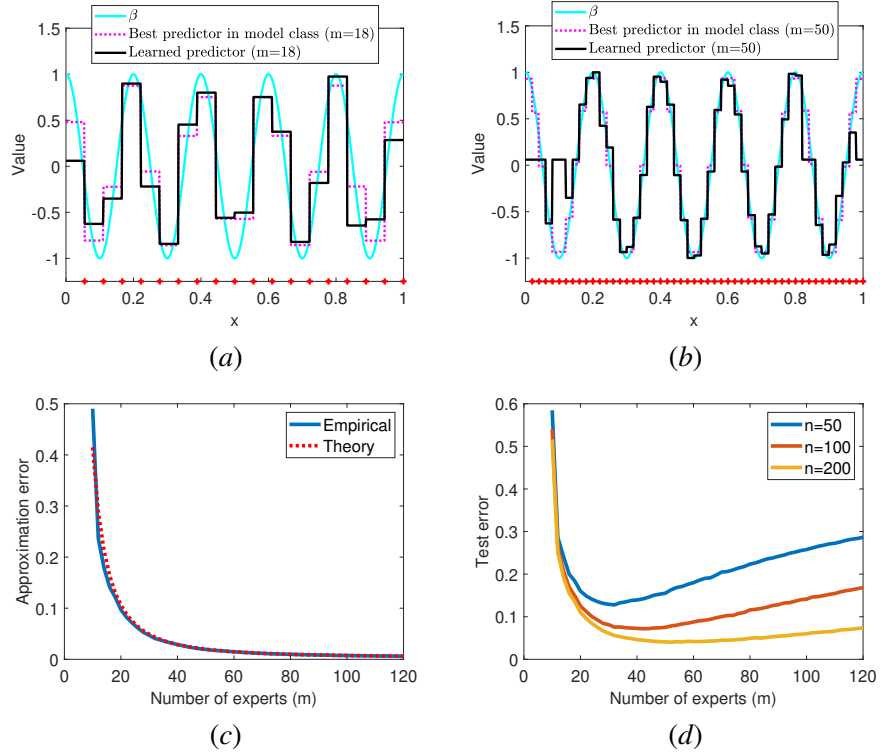


Figure 3: Examples for **learning experts for uniform segmentation**. This experiment is for a **c**o-sine β and truncated Gaussian p_x from Figs. 1(a), 1(c), respectively. Here, in (a)-(b), the red markers on the x -axis denote the given uniform segmentation points $\{a_i = \frac{i}{m}\}_{i=1}^m$; the dotted magenta lines show the best predictor in $\mathcal{H}_{m,1}^c$ ($\{a_i = \frac{i}{m}\}_{i=1}^m$); the black lines show the predictor learned from a training data of 200 examples. (c) shows the empirical and theoretical approximation error curves of the best predictors in $\mathcal{H}_{m,1}^c$ ($\{a_i = \frac{i}{m}\}_{i=1}^m$). (d) shows the empirical test error curves for the learned predictors for three sizes of training dataset.

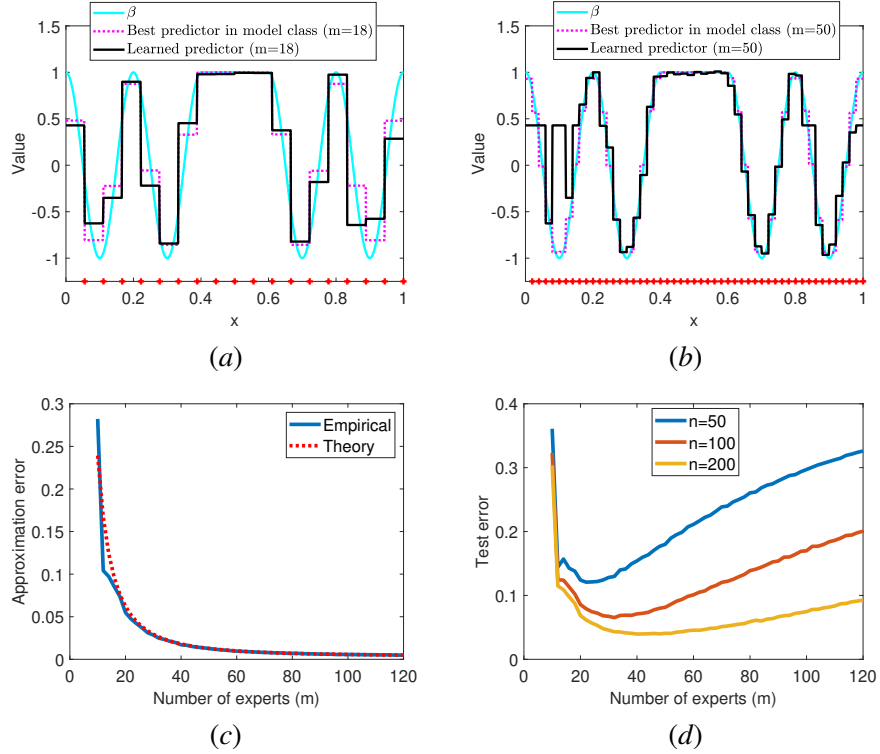


Figure 4: Examples for **learning experts for uniform segmentation**. This experiment is for a **cosine with a constant segment** β and truncated Gaussian p_x from Figs. 2(a), 2(c), respectively. Here, in (a)-(b), the red markers on the x -axis denote the given uniform segmentation points $\{a_i = \frac{i}{m}\}_{i=1}^m$; the dotted magenta lines show the best predictor in $\mathcal{H}_{m,1}^c$ ($\{a_i = \frac{i}{m}\}_{i=1}^m$); the black lines show the predictor learned from a training data of 200 examples. (c) shows the empirical and theoretical approximation error curves of the best predictors in $\mathcal{H}_{m,1}^c$ ($\{a_i = \frac{i}{m}\}_{i=1}^m$). (d) shows the empirical test error curves for the learned predictors for three sizes of training dataset.

7. Conclusion

This paper has established a new quantization-based analysis approach for MoE learning. The proposed approach uses high-rate quantization theory principles by assuming that the MoE has many constant experts, each uniquely responsible for an input-space region. These regions are assumed to be sufficiently small to allow the analysis of the discrete segmentation to regions as a continuous density, leading to a continuous analysis of the approximation error of the MoE model class for when both the experts and segmentation are learnable parameters and when only the experts are learnable parameters for a given segmentation. Moreover, our analysis eventually shows the tradeoff between the approximation error and the estimation error for MoE with learnable experts for a given segmentation. This paper paves the way for future research to examine the estimation error of learning the input-space segmentation, and to study more complex MoE models such as with other sparsity levels and non-constant experts.

References

E. S. Barnes and N. J. A. Sloane. The optimal lattice quantizer in three dimensions. *SIAM Journal on Algebraic Discrete Methods*, 4(1):30–41, 1983.

W. R. Bennett. Spectra of quantized signals. *The Bell System Technical Journal*, 27(3):446–472, 1948.

Y. Dar and A. M. Bruckstein. On high-resolution adaptive sampling of deterministic signals. *Journal of Mathematical Imaging and Vision*, 61(7):944–966, 2019.

Q. Du and D. Wang. The optimal centroidal voronoi tessellations and the gersho’s conjecture in the three-dimensional space. *Computers & Mathematics with Applications*, 49(9):1355–1373, 2005.

W. Fedus, J. Dean, and B. Zoph. A review of sparse expert models in deep learning. *arXiv preprint arXiv:2209.01667*, 2022a.

W. Fedus, B. Zoph, and N. Shazeer. Switch transformers: Scaling to trillion parameter models with simple and efficient sparsity. *Journal of Machine Learning Research*, 23(120):1–39, 2022b.

L. Fejes Toth. Sur la représentation d’une population infinie par un nombre fini d’éléments. *Acta Mathematica Academiae Scientiarum Hungarica*, 10:299–304, 1959.

A. Gersho. Asymptotically optimal block quantization. *IEEE Transactions on Information Theory*, 25(4):373–380, 1979.

R. M. Gray and D. L. Neuhoff. Quantization. *IEEE Transactions on Information Theory*, 44(6): 2325–2383, 1998.

S. Jelassi, C. Mohri, D. Brandfonbrener, A. Gu, N. Vyas, N. Anand, D. Alvarez-Melis, Y. Li, S. M. Kakade, and E. Malach. Mixture of parrots: Experts improve memorization more than reasoning. In *International Conference on Learning Representations*, 2025.

P. Jin, B. Zhu, L. Yuan, and S. Yan. MoE++: Accelerating mixture-of-experts methods with zero-computation experts. *arXiv preprint arXiv:2410.07348*, 2024.

D. P. Kingma and M. Welling. Auto-encoding variational Bayes. In *International Conference on Learning Representations (ICLR)*, 2014.

A. Liu, B. Feng, B. Wang, B. Wang, B. Liu, C. Zhao, C. Dengr, C. Ruan, D. Dai, D. Guo, et al. DeepSeek-v2: A strong, economical, and efficient mixture-of-experts language model. *arXiv preprint arXiv:2405.04434*, 2024.

S. Lloyd. Least squares quantization in PCM. *IEEE Transactions on Information Theory*, 28(2):129–137, 1982.

S. Na and D. L. Neuhoff. Bennett’s integral for vector quantizers. *IEEE Transactions on Information Theory*, 41(4):886–900, 1995.

D. Newman. The hexagon theorem. *IEEE Transactions on Information Theory*, 28(2):137–139, 1982.

H. Nguyen, T. Nguyen, and N. Ho. Demystifying softmax gating function in gaussian mixture of experts. In *Advances in Neural Information Processing Systems*, pages 4624–4652, 2023.

H. Nguyen, P. Akbarian, F. Yan, and N. Ho. Statistical perspective of top-K sparse softmax gating mixture of experts. In *International Conference on Learning Representations*, 2024a.

H. Nguyen, N. Ho, and A. Rinaldo. On least square estimation in softmax gating mixture of experts. In *International Conference on Machine Learning*, 2024b.

H. Nguyen, N. Ho, and A. Rinaldo. Sigmoid gating is more sample efficient than softmax gating in mixture of experts. In *Advances in Neural Information Processing Systems*, volume 37, pages 118357–118388, 2024c.

H. Nguyen, T. Nguyen, K. Nguyen, and N. Ho. Towards convergence rates for parameter estimation in Gaussian-gated mixture of experts. In *International Conference on Artificial Intelligence and Statistics*, volume 238, pages 2683–2691, 2024d.

P. F. Panter and W. Dite. Quantization distortion in pulse-count modulation with nonuniform spacing of levels. *Proceedings of the IRE*, 39(1):44–48, 1951.

C. Riquelme, J. Puigcerver, B. Mustafa, M. Neumann, R. Jenatton, A. Susano Pinto, D. Keysers, and N. Houlsby. Scaling vision with sparse mixture of experts. In *Advances in Neural Information Processing Systems (NeurIPS)*, 2021.

S. Shalev-Shwartz and S. Ben-David. *Understanding machine learning: From theory to algorithms*. Cambridge university press, 2014.

N. Shazeer, A. Mirhoseini, K. Maziarz, A. Davis, Q. Le, G. Hinton, and J. Dean. Outrageously large neural networks: The sparsely-gated mixture-of-experts layer. In *International Conference on Learning Representations (ICLR)*, 2017.

R. Vershynin. *High-Dimensional Probability: An Introduction with Applications in Data Science*. Cambridge University Press, 2018.

P. Zador. Asymptotic quantization error of continuous signals and the quantization dimension. *IEEE Transactions on Information Theory*, 28(2):139–149, 1982.

R. Zamir and M. Feder. On lattice quantization noise. *IEEE Transactions on Information Theory*, 42(4):1152–1159, 1996.

J. Zhao, P. Wang, J. Yang, R. Cai, G. Liu, J. Srinivasa, R. R. Kompella, Y. Liang, and Z. Wang. Sparse mixture-of-experts for compositional generalization: Empirical evidence and theoretical foundations of optimal sparsity. *arXiv preprint arXiv:2410.13964*, 2024.

Appendix A. High Rate Quantization: Formulations from Related Work

This appendix provides a brief overview of some formulations and assumptions from the high-rate quantization literature. This should help to compare the formulations between the standard quantization problem and our MoE learning problem. For more details see the overview by [Gray and Neuhoff \(1998\)](#).

A.1. Scalar High-Rate Quantization: Approximated Error Formula

Consider scalar quantization for a random input x drawn from the probability distribution function p_x over $[0, 1]$. The quantizer design requires to segment the input space $[0, 1]$ to m intervals $\{[a_{i-1}, a_i]\}_{i=1}^m$ where $0 = a_0 < a_1 < \dots < a_{m-1} < a_m = 1$; formally, the m^{th} interval is $[a_{m-1}, a_m]$ but for writing simplicity it will be written as $[a_{m-1}, a_m)$ as the other intervals. Each interval has a unique representation value: $v_i, \forall i \in \{1, \dots, m\}$. The quantizer function can be written as $Q(x) = v_i$ for $x \in [a_{i-1}, a_i)$. The performance criterion is the expected squared error

$$\mathcal{E}_Q = \mathbb{E}_x \left[(Q(x) - x)^2 \right] = \sum_{i=1}^m \int_{x=a_{i-1}}^{a_i} (v_i - x)^2 p_x(x) dx. \quad (42)$$

Under the high-rate quantization assumption, m is large such that the intervals are sufficiently small and p_x is approximately constant within each of them, i.e.,

$$p_x(x) \approx p_x(x_i) \text{ for } x \in [a_{i-1}, a_i) \quad (43)$$

where $x_i \triangleq \frac{a_{i-1}+a_i}{2}$ is the center of the i^{th} interval. This implies that, for a given segmentation, the optimal representation values are the interval centers, i.e.,

$$v_i = x_i, \forall i \in \{1, \dots, m\}. \quad (44)$$

Based on these, the high-rate quantization literature uses the approximated error formula:

$$\mathcal{E}_Q \approx \frac{1}{12m^2} \int_{x=0}^1 \frac{p_x(x)}{g^2(x)} dx \quad (45)$$

where the smooth function g has the following meanings:

- In the compander design that turns a uniform quantizer (whose intervals have equal length) into a nonuniform one (Bennett, 1948; Panter and Dite, 1951), g is the derivative of a nonlinear function which is applied as a preprocessing and its inverse as postprocessing to a uniform quantizer. Namely, if Q_{unif} is a uniform quantizer over $[0, 1]$ whose quantization interval length is $\frac{1}{m}$, a nonuniform quantizer can be formed by $Q(x) = v(Q_{\text{unif}}(u(x)))$ where u is a preprocessing function (called compressor) and its inverse is the postprocessing function v (called expander). In (45) we have $g(x) = u'(x)$.
- For nonuniform quantizers in general (i.e., also beyond the compander design), Lloyd (1982) defined g as the density of quantization intervals.

It was importantly shown by Panter and Dite (1951) that the quantization error (45) is minimized by

$$g^{\text{opt}}(x) = \frac{\sqrt[3]{p_x(x)dx}}{\int_{\xi=0}^1 \sqrt[3]{p_x(\xi)d\xi}} \quad (46)$$

which attains the minimal quantization error of

$$\mathcal{E}_Q^{\text{opt}} \approx \frac{1}{12m^2} \left(\int_{x=0}^1 \sqrt[3]{p_x(x)dx} \right)^3. \quad (47)$$

A.2. Scalar High-Rate Quantization: Forming a Quantizer from a Quantization Segment Density

In the compander design (Bennett, 1948; Panter and Dite, 1951), the optimal compressor function is obtained by integrating g^{opt} from (46):

$$u(x) = \int_{\xi=0}^x g^{\text{opt}}(\xi)d\xi = \frac{\int_{\xi=0}^x g^{\text{opt}}(\xi)d\xi}{\int_{\xi=0}^1 g^{\text{opt}}(\xi)d\xi}. \quad (48)$$

The compander design requires also an expander function v , which is the inverse of the compressor u from (48):

$$\int_{\xi=0}^{v(x)} g^{\text{opt}}(\xi)d\xi = x. \quad (49)$$

The equation (49) has a unique solution when g^{opt} is positive over $[0, 1]$, here this requires that p_x is positive over $[0, 1]$; this will make the compressor function strictly monotonic increasing and therefore invertible.

More generally than the compander design, the optimal quantization intervals (i.e., optimal segmentation of the input space $[0, 1]$) are defined by the optimal expander from (49) as

$$a_i^{\text{opt}} = v\left(\frac{i}{m}\right), \quad \forall i \in \{1, \dots, m\}. \quad (50)$$

Importantly, for the multidimensional case of vector quantizers, it is generally impossible to form the optimal segmentation by extending (48)-(50); this is because multidimensional quantization regions are defined by their shapes and not just by their volumes.

More explanations about the multidimensional case of vector quantizers are provided throughout our multidimensional MoE learning analysis in Section 5 and Appendix C; for more details see Section 2.2 and the detailed overview by [Gray and Neuhoff \(1998\)](#).

Appendix B. Related Work: Gersho's Conjecture for High-Rate Vector Quantization

Gersho's conjecture is true when the d -dimensional space can be optimally tessellated by a lattice, i.e., by one optimal polytope; this is known to hold for $d = 1$ by intervals, for $d = 2$ by hexagons ([Fejes Toth, 1959](#); [Newman, 1982](#)). For $d = 3$, it is informally believed that the optimal tessellation is the body-centered cubic lattice, which was proved as the optimal lattice tessellation ([Barnes and Sloane, 1983](#); [Du and Wang, 2005](#)). For $d \geq 3$, it is unknown if the optimal tessellation is by lattice and if Gersho's conjecture is accurate. Yet, as explained by [Gray and Neuhoff \(1998\)](#), considering the relation between the conjecture to an unspecified constant from the rigorous theory by [Zador \(1982\)](#), the conjecture inaccuracy for $d \geq 3$ is not expected to significantly affect the approximated error; moreover, a theoretical result by [Zamir and Feder \(1996\)](#) implies that the conjecture inaccuracy vanishes as $d \rightarrow \infty$. A detailed discussion on the conjecture is given by [Gray and Neuhoff \(1998\)](#). All of these established Gersho's conjecture as a useful tool for high-rate vector quantization theory; in Appendix C we use this conjecture to theoretically analyze the segmentation that minimizes the test error upper bound of mixture of many experts for multidimensional inputs.

Appendix C. MoE for Multidimensional Inputs: The Expert Segment Density that Minimizes the Test-Error Upper Bound

To proceed from the point where Section 5 ends, we use a widely-believed conjecture for high-rate vector quantization by [Gersho \(1979\)](#); see Section 2.2, Appendix B and ([Gray and Neuhoff, 1998](#)) for more details.

Assumption 5 *The large number of experts and the small region assumption induce regions whose shapes are approximately congruent to the optimal convex polytope $A_{\text{opt},d}$ that tessellates the d -dimensional space. Accordingly,*

$$\mu(\mathbf{x}) \approx M(A_{\text{opt},d}) \quad (51)$$

for any $\mathbf{x} \in [0, 1]^d$.

Here, this assumption leads to the following test error bound for the multidimensional MoE.

Corollary 12 *Under Assumption 5, the approximation of the upper bound from (30) is*

$$\tilde{\mathcal{E}}_{\text{test}}^{\text{bound}} = \sigma_\epsilon^2 + \frac{d \cdot M(A_{\text{opt},d})}{m^{2/d}} \int_{\mathbf{x} \in [0, 1]^d} \frac{\|\nabla \beta(\mathbf{x})\|_2^2 p_{\mathbf{x}}(\mathbf{x})}{\lambda^{2/d}(\mathbf{x})} d\mathbf{x}. \quad (52)$$

Then, the following theorem provides the upper-bound minimizing (UBM) expert segment density function λ^{UBM} and its corresponding error bound. Note that (52) is an upper bound for the approximation error \mathcal{E}_{app} of the hypothesis class $\mathcal{H}_{m,d}^c(\{A_i\}_{i=1}^m)$.

Theorem 13 *The test error's upper bound $\tilde{\mathcal{E}}_{\text{test}}^{\text{bound}}$ from (52) is minimized by the expert segment density function*

$$\lambda^{\text{UBM}}(\mathbf{x}) = \frac{\left(p_{\mathbf{x}}(\mathbf{x}) \|\nabla \beta(\mathbf{x})\|_2^2 \right)^{\frac{d}{d+2}}}{\int_{\boldsymbol{\xi} \in [0,1]^d} \left(p_{\mathbf{x}}(\boldsymbol{\xi}) \|\nabla \beta(\boldsymbol{\xi})\|_2^2 \right)^{\frac{d}{d+2}} d\boldsymbol{\xi}} \quad (53)$$

that attains the minimal upper bound of the test error:

$$\tilde{\mathcal{E}}_{\text{test}}^{\text{bound,min}} = \sigma_{\epsilon}^2 + \frac{d \cdot M(A_d^{\text{opt}})}{m^{2/d}} \left(\int_{\mathbf{x} \in [0,1]^d} \left(p_{\mathbf{x}}(\mathbf{x}) \|\nabla \beta(\mathbf{x})\|_2^2 \right)^{\frac{d}{d+2}} d\mathbf{x} \right)^{1+\frac{2}{d}}. \quad (54)$$

The theorem proof is provided in Appendix F.3.

The segment density in (53) minimizes the upper bound of the test error, and does not directly minimize the test error. Optimizing an objective's bound is a valid heuristic approach for when the objective optimization is intractable (e.g., as commonly done for variational autoencoders (Kingma and Welling, 2014)); the assumption is that minimization of the objective's upper bound would promote minimization of the true objective. However, usually the upper-bound minimizing solution does not achieve the minimum of the true objective. An important aspect of Theorem 13 is the connection to the corresponding results for high-rate vector quantization by Gersho (1979); Na and Neuhoff (1995).

Regardless to the suboptimality due to minimizing an upper bound, there is an important difference between the multidimensional and one-dimensional cases. in the one-dimensional case, it is possible to form an optimal segmentation from the optimal segment density function (whose values are positive over the entire input domain, see Appendix A.2); but in the multidimensional case, it is usually impossible to form an optimal segmentation from the optimal segment density function due to the ambiguity in the optimal shapes of the segmentation regions. More detailed discussions on this appear in the high-rate vector quantization literature (Gersho, 1979; Na and Neuhoff, 1995; Gray and Neuhoff, 1998).

Appendix D. Proofs for Section 3

D.1. Proof of the Test Error Formula for Multidimensional MoE in Eq. (7)

The following proof is based on the data model (1) and the MoE predictor form (2).

$$\begin{aligned}
 \mathcal{E}_{\text{test}} &= \mathbb{E}_{\mathbf{x}, y} \left[\left(\hat{\beta}(\mathbf{x}) - y \right)^2 \right] \tag{55} \\
 &= \mathbb{E}_{\mathbf{x}, \epsilon} \left[\left(\hat{\beta}(\mathbf{x}) - \beta(\mathbf{x}) - \epsilon \right)^2 \right] \\
 &= \sigma_{\epsilon}^2 + \mathbb{E}_{\mathbf{x}} \left[\left(\hat{\beta}(\mathbf{x}) - \beta(\mathbf{x}) \right)^2 \right] \\
 &= \sigma_{\epsilon}^2 + \int_{\mathbf{x} \in [0,1]^d} \left(\hat{\beta}(\mathbf{x}) - \beta(\mathbf{x}) \right)^2 p_{\mathbf{x}}(\mathbf{x}) d\mathbf{x} \\
 &= \sigma_{\epsilon}^2 + \sum_{i=1}^m \int_{\mathbf{x} \in A_i} (c_i - \beta(\mathbf{x}))^2 p_{\mathbf{x}}(\mathbf{x}) d\mathbf{x}.
 \end{aligned}$$

D.2. Proof of the Optimal Constants in Eq. (9)

For a given segmentation $\{A_i\}_{i=1}^m$, the optimal constants $\{c_i^{\text{opt}}\}_{i=1}^m$ are defined by the minimization problem:

$$\{c_i^{\text{opt}}\}_{i=1}^m = \arg \min_{\{c_i\}_{i=1}^m \in \mathbb{R}} \mathcal{E}_{\text{test}} (\{A_i\}_{i=1}^m, \{c_i\}_{i=1}^m) \tag{56}$$

$$= \arg \min_{\{c_i\}_{i=1}^m \in \mathbb{R}} \sum_{i=1}^m \int_{\mathbf{x} \in A_i} (c_i - \beta(\mathbf{x}))^2 p_{\mathbf{x}}(\mathbf{x}) d\mathbf{x}. \tag{57}$$

This is a convex minimization problem; hence, the optimal constants satisfy

$$\frac{\partial}{\partial c_i} \mathcal{E}_{\text{test}} (\{A_i\}_{i=1}^m, \{c_i\}_{i=1}^m) = 0, \quad \forall i \in \{1, \dots, m\} \tag{58}$$

Our test error formula (7) implies that

$$\frac{\partial}{\partial c_i} \mathcal{E}_{\text{test}} (\{A_i\}_{i=1}^m, \{c_i\}_{i=1}^m) = \int_{\mathbf{x} \in A_i} 2(c_i - \beta(\mathbf{x})) p_{\mathbf{x}}(\mathbf{x}) d\mathbf{x}, \tag{59}$$

and, therefore, (58) implies

$$c_i^{\text{opt}} = \frac{\int_{\mathbf{x} \in A_i} \beta(\mathbf{x}) p_{\mathbf{x}}(\mathbf{x}) d\mathbf{x}}{\int_{\mathbf{x} \in A_i} p_{\mathbf{x}}(\mathbf{x}) d\mathbf{x}}, \quad \forall i \in \{1, \dots, m\}, \tag{60}$$

which proves (9).

Appendix E. Proofs for the Case of One-Dimensional Inputs

E.1. Proof of Theorem 1: The Optimal Constants and Test Error in Sum Form using Locally-Linear Approximations for One-Dimensional Inputs

For a start, note that the first-order Taylor approximation of β and p_x from (16) and (17) imply the approximation of their product as

$$\beta(x)p_x(x) = \beta(x_i)p_x(x_i) + (\beta'(x_i)p_x(x_i) + p'_x(x_i)\beta(x_i)) \cdot (x - x_i) + o(|x - x_i|). \quad (61)$$

Then, setting the approximations (17), (61) into (15) gives

$$\begin{aligned} c_i^{\text{opt}} &= \frac{\int_{x=a_{i-1}}^{a_i} (\beta(x_i)p_x(x_i) + (\beta'(x_i)p_x(x_i) + p'_x(x_i)\beta(x_i)) \cdot (x - x_i) + o(|x - x_i|)) dx}{\int_{x=a_{i-1}}^{a_i} (p_x(x_i) + p'_x(x_i) \cdot (x - x_i) + o(|x - x_i|)) dx} \\ &= \frac{\beta(x_i)p_x(x_i)\Delta_i + o(\Delta_i^2)}{p_x(x_i)\Delta_i + o(\Delta_i^2)} \end{aligned} \quad (62)$$

where the following basic results were used:

$$\int_{x=a_{i-1}}^{a_i} dx = \Delta_i \quad (63)$$

$$\int_{x=a_{i-1}}^{a_i} (x - x_i) dx = 0 \quad (64)$$

$$\int_{x=a_{i-1}}^{a_i} o(|x - x_i|) dx \in o(\Delta_i^2) \text{ as } \Delta_i \rightarrow 0. \quad (65)$$

The proof of (65) is based on the little-o definition: $f(x) \in o(|x - x_i|)$ as $x \rightarrow x_i$ implies $\lim_{x \rightarrow x_i} \frac{f(x)}{|x - x_i|} = 0$ and that for every $\varepsilon > 0$ there exists a $\delta > 0$ such that $|x - x_i| \in (0, \delta)$ implies $\left| \frac{f(x)}{|x - x_i|} \right| < \varepsilon$ and hence $|f(x)| < \varepsilon|x - x_i|$. For an interval length $\Delta_i > 0$ we have $a_i = x_i + \frac{\Delta_i}{2}$ and $a_{i-1} = x_i - \frac{\Delta_i}{2}$, then our integration over $x \in [a_{i-1}, a_i]$ and the requirement $|x - x_i| \in (0, \delta)$ imply that $\frac{\Delta_i}{2} \in (0, \delta)$. Accordingly,

$$\begin{aligned} \left| \int_{x=a_{i-1}}^{a_i} o(|x - x_i|) dx \right| &= \left| \int_{x=x_i - \frac{\Delta_i}{2}}^{x_i + \frac{\Delta_i}{2}} o(|x - x_i|) dx \right| \leq \int_{x=x_i - \frac{\Delta_i}{2}}^{x_i + \frac{\Delta_i}{2}} |o(|x - x_i|)| dx \\ &< \int_{x=x_i - \frac{\Delta_i}{2}}^{x_i + \frac{\Delta_i}{2}} \varepsilon|x - x_i| dx = 2\varepsilon \int_{x=x_i}^{x_i + \frac{\Delta_i}{2}} (x - x_i) dx = \varepsilon \frac{\Delta_i^2}{4} \end{aligned} \quad (66)$$

that implies

$$\frac{\left| \int_{x=a_{i-1}}^{a_i} o(|x - x_i|) dx \right|}{\Delta_i^2} < \frac{\varepsilon}{4} \quad (67)$$

which holds for every $\varepsilon > 0$ and its existing $\delta > 0$ that were defined above. Recall that $\frac{\Delta_i}{2} \in (0, \delta)$. Consequently, we get (65).

We return to (62) to further develop it:

$$c_i^{\text{opt}} = \frac{p_x(x_i)\Delta_i(\beta(x_i) + o(\Delta_i))}{p_x(x_i)\Delta_i(1 + o(\Delta_i))} = \frac{\beta(x_i) + o(\Delta_i)}{1 + o(\Delta_i)} \quad (68)$$

$$= (1 + o(\Delta_i))(\beta(x_i) + o(\Delta_i)) \quad (69)$$

$$= \beta(x_i) + o(\Delta_i) \quad (70)$$

where (69) is due to the little-o property: if $f(x) \in o(1)$ then $\frac{1}{1+o(f(x))} = 1 + o(f(x))$. By this, we complete the proof of (18) in Theorem 1.

The proof of the error formula (19) in Theorem 1 is by setting the linear approximations (16)-(17) and the optimal constants for small subintervals (18) in the error formula (14):

$$\begin{aligned} \mathcal{E}_{\text{test}}(\{a_i\}_{i=0}^m, \{c_i^{\text{opt}}\}_{i=1}^m) &= \quad (71) \\ &= \sigma_\epsilon^2 + \sum_{i=1}^m \int_{x=a_{i-1}}^{a_i} (\beta(x_i) + o(\Delta_i) - (\beta(x_i) + \beta'(x_i) \cdot (x - x_i) + R_{\beta,1}(x)))^2 \\ &\quad \cdot (p_x(x_i) + p'_x(x_i) \cdot (x - x_i) + R_{p_x,1}(x)) \, dx \\ &= \sigma_\epsilon^2 + \\ &\quad \sum_{i=1}^m \int_{x=a_{i-1}}^{a_i} (\beta'(x_i) \cdot (x - x_i) + R_{\beta,1}(x) + o(\Delta_i))^2 (p_x(x_i) + p'_x(x_i) \cdot (x - x_i) + R_{p_x,1}(x)) \, dx \\ &= \sigma_\epsilon^2 + \sum_{i=1}^m \left(o(\Delta_i^3) + (\beta'(x_i))^2 \int_{x=a_{i-1}}^{a_i} (x - x_i)^2 (p_x(x_i) + p'_x(x_i) \cdot (x - x_i)) \, dx \right) \\ &= \sigma_\epsilon^2 + \sum_{i=1}^m \left(o(\Delta_i^3) + (\beta'(x_i))^2 p_x(x_i) \int_{x=a_{i-1}}^{a_i} (x - x_i)^2 \, dx \right) \\ &= \sigma_\epsilon^2 + \sum_{i=1}^m \left(o(\Delta_i^3) + (\beta'(x_i))^2 p_x(x_i) \cdot \frac{\Delta_i^3}{12} \right) \\ &= \sigma_\epsilon^2 + \sum_{i=1}^m \left((\beta'(x_i))^2 p_x(x_i) \cdot \frac{\Delta_i^3}{12} \right) + o(\Delta_{\max}^3) \end{aligned}$$

where $\Delta_{\max} = \max_{i \in \{1, \dots, m\}} \Delta_i$ is the largest subinterval. The developments in (71) use (64) as well as

$$\int_{x=a_{i-1}}^{a_i} (x - x_i)^3 \, dx = 0 \quad (72)$$

$$\int_{x=a_{i-1}}^{a_i} o(|x - x_i|^2) \, dx \in o(\Delta_i^3) \quad \text{as } \Delta_i \rightarrow 0. \quad (73)$$

where (73) can be proved similarly to (65). By this we conclude the proof of the test error formula (19) and Theorem 1.

E.2. Additional Details on Corollary 2

Starting from the test error formula (19), we omit the explicit inaccuracy term $o(\Delta_{\max}^3)$ and develop as follows:

$$\begin{aligned}\mathcal{E}_{\text{test}} &\approx \sigma_{\epsilon}^2 + \frac{1}{12} \sum_{i=1}^m (\beta'(x_i))^2 p_{\mathbf{x}}(x_i) \Delta_i^3 \\ &\approx \sigma_{\epsilon}^2 + \frac{1}{12} \sum_{i=1}^m (\beta'(x_i))^2 p_{\mathbf{x}}(x_i) \frac{1}{m^2 \lambda^2(x_i)} \Delta_i \\ &\approx \sigma_{\epsilon}^2 + \frac{1}{12m^2} \int_{x=0}^1 \frac{(\beta'(x))^2 p_{\mathbf{x}}(x)}{\lambda^2(x)} dx \\ &\triangleq \tilde{\mathcal{E}}_{\text{test}}.\end{aligned}\quad (74)$$

The developments in (74) use Assumption 1 and approximation of the sum as integral due to the small segment assumption.

E.3. Proof of Theorem 3: The Optimal Expert Segment Density and the Corresponding Test Error

Let us develop a lower bound for the integral $\int_{x=0}^1 \frac{(\beta'(x))^2 p_{\mathbf{x}}(x)}{\lambda^2(x)} dx$ from the test error formula of Corollary 2. By Hölder's inequality,

$$\begin{aligned}\left(\int_{x=0}^1 \left(\sqrt[3]{(\beta'(x))^2 p_{\mathbf{x}}(x)} \frac{1}{\lambda^{2/3}(x)} \right)^3 dx \right)^{1/3} &\left(\int_{x=0}^1 \left(\lambda^{2/3}(x) \right)^{3/2} dx \right)^{2/3} \\ &\geq \int_{x=0}^1 \sqrt[3]{(\beta'(x))^2 p_{\mathbf{x}}(x)} dx\end{aligned}\quad (75)$$

where the left side can be simplified, thus,

$$\left(\int_{x=0}^1 (\beta'(x))^2 p_{\mathbf{x}}(x) \frac{1}{\lambda^2(x)} dx \right)^{1/3} \left(\int_{x=0}^1 \lambda(x) dx \right)^{2/3} \geq \int_{x=0}^1 \sqrt[3]{(\beta'(x))^2 p_{\mathbf{x}}(x)} dx. \quad (76)$$

The density $\lambda(x)$ integrates to 1, i.e., $\int_{x=0}^1 \lambda(x) dx = 1$, hence, we get that

$$\int_{x=0}^1 (\beta'(x))^2 p_{\mathbf{x}}(x) \frac{1}{\lambda^2(x)} dx \geq \left(\int_{x=0}^1 \sqrt[3]{(\beta'(x))^2 p_{\mathbf{x}}(x)} dx \right)^3 \quad (77)$$

where the left side is the integral from the test error formula of Corollary 2.

Hölder's inequality in (75) is attained with equality if $\lambda(x)$ is linearly proportional to $(\beta'(x))^2 p_{\mathbf{x}}(x) \frac{1}{\lambda^2(x)}$. Namely, for a constant ζ such that

$$\lambda(x) = \zeta \cdot (\beta'(x))^2 p_{\mathbf{x}}(x) \frac{1}{\lambda^2(x)} \quad (78)$$

which, using integration over $[0, 1]$ and that the density integrates to 1, implies that

$$\zeta = \frac{1}{\left(\int_{x=0}^1 \sqrt[3]{(\beta'(x))^2 p_x(x)} dx \right)^3}. \quad (79)$$

Consequently, the density that minimizes the integral in the left side of (77) is

$$\lambda^{\text{opt}}(x) = \frac{\sqrt[3]{p_x(x) (\beta'(x))^2}}{\int_{\xi=0}^1 \sqrt[3]{p_x(\xi) (\beta'(\xi))^2} d\xi}. \quad (80)$$

The optimal density $\lambda^{\text{opt}}(x)$ makes (77) to hold with equality. Then, plugging the right side of (77) into the test error formula of Corollary 2 gives the minimal test error of

$$\tilde{\mathcal{E}}_{\text{test}}^{\text{opt}} = \sigma_{\epsilon}^2 + \frac{1}{12m^2} \left(\int_{x=0}^1 \sqrt[3]{p_x(x) (\beta'(x))^2} dx \right)^3. \quad (81)$$

This completes the proof of Theorem 3.

Appendix F. Proofs for the Case of Multidimensional Inputs

F.1. Proof of Theorem 4: The Optimal Constants and Test Error in Sum Form using Locally-Linear Approximations for Multidimensional Inputs

For a start, note that the first-order Taylor approximation of β and p_x from (25) and (26) imply the approximation of their product as

$$\beta(\mathbf{x})p_x(\mathbf{x}) = \beta(\mathbf{x}_i)p_x(\mathbf{x}_i) + (\beta(\mathbf{x}_i)\nabla p_x(\mathbf{x}_i) + p_x(\mathbf{x}_i)\nabla\beta(\mathbf{x}_i))^T(\mathbf{x} - \mathbf{x}_i) + o(\|\mathbf{x} - \mathbf{x}_i\|_2). \quad (82)$$

Then, setting the approximations (26), (82) into (9) gives

$$\begin{aligned} c_i^{\text{opt}} &= \frac{\int_{\mathbf{x} \in A_i} \left(\beta(\mathbf{x}_i)p_x(\mathbf{x}_i) + (\beta(\mathbf{x}_i)\nabla p_x(\mathbf{x}_i) + p_x(\mathbf{x}_i)\nabla\beta(\mathbf{x}_i))^T(\mathbf{x} - \mathbf{x}_i) + o(\|\mathbf{x} - \mathbf{x}_i\|_2) \right) d\mathbf{x}}{\int_{\mathbf{x} \in A_i} (p_x(\mathbf{x}_i) + \nabla p_x(\mathbf{x}_i)^T(\mathbf{x} - \mathbf{x}_i) + o(\|\mathbf{x} - \mathbf{x}_i\|_2)) d\mathbf{x}} \\ &= \frac{\beta(\mathbf{x}_i)p_x(\mathbf{x}_i)V(A_i) + o\left(V(A_i)^{1+\frac{1}{d}}\right)}{p_x(\mathbf{x}_i)V(A_i) + o\left(V(A_i)^{1+\frac{1}{d}}\right)} \end{aligned} \quad (83)$$

where the following basic results were used:

$$\int_{\mathbf{x} \in A_i} d\mathbf{x} = V(A_i) \quad (84)$$

$$\int_{\mathbf{x} \in A_i} (\mathbf{x} - \mathbf{x}_i) d\mathbf{x} = 0 \quad (85)$$

$$\int_{\mathbf{x} \in A_i} o(\|\mathbf{x} - \mathbf{x}_i\|_2) d\mathbf{x} \in o\left(V(A_i)^{1+\frac{1}{d}}\right) \text{ as } V(A_i) \rightarrow 0. \quad (86)$$

The proof of (86) is based on the little-o definition: $f(\mathbf{x}) \in o(\|\mathbf{x} - \mathbf{x}_i\|_2)$ as $\mathbf{x} \rightarrow \mathbf{x}_i$ implies $\lim_{\mathbf{x} \rightarrow \mathbf{x}_i} \frac{f(\mathbf{x})}{\|\mathbf{x} - \mathbf{x}_i\|_2} = 0$ and that for every $\varepsilon > 0$ there exists a $\delta > 0$ such that $\|\mathbf{x} - \mathbf{x}_i\|_2 \in (0, \delta)$ implies $\left| \frac{f(\mathbf{x})}{\|\mathbf{x} - \mathbf{x}_i\|_2} \right| < \varepsilon$ and hence $|f(\mathbf{x})| < \varepsilon \|\mathbf{x} - \mathbf{x}_i\|_2$. Recall that \mathbf{x}_i is the center of the region A_i and that we are interested in integration over $\mathbf{x} \in A_i$. Accordingly,

$$\begin{aligned} \left| \int_{\mathbf{x} \in A_i} o(\|\mathbf{x} - \mathbf{x}_i\|_2) d\mathbf{x} \right| &\leq \int_{\mathbf{x} \in A_i} |o(\|\mathbf{x} - \mathbf{x}_i\|_2)| d\mathbf{x} \\ &< \int_{\mathbf{x} \in A_i} \varepsilon \|\mathbf{x} - \mathbf{x}_i\|_2 d\mathbf{x}. \end{aligned} \quad (87)$$

Using the definition of the normalized k^{th} moment of inertia,

$$M_k(A_i) \triangleq \frac{\int_{\mathbf{x} \in A_i} \|\mathbf{x} - \mathbf{x}_i\|_2^k d\mathbf{x}}{d \cdot V(A_i)^{1+\frac{k}{d}}} \quad (88)$$

for $k = 1$, we get $\int_{\mathbf{x} \in A_i} \|\mathbf{x} - \mathbf{x}_i\|_2 d\mathbf{x} = M_1(A_i) \cdot d \cdot V(A_i)^{1+\frac{1}{d}}$ and set it in (87) to yield

$$\left| \int_{\mathbf{x} \in A_i} o(\|\mathbf{x} - \mathbf{x}_i\|_2) d\mathbf{x} \right| < \varepsilon M_1(A_i) \cdot d \cdot V(A_i)^{1+\frac{1}{d}}, \quad (89)$$

i.e.,

$$\frac{\left| \int_{\mathbf{x} \in A_i} o(\|\mathbf{x} - \mathbf{x}_i\|_2) d\mathbf{x} \right|}{V(A_i)^{1+\frac{1}{d}}} < \varepsilon M_1(A_i) \cdot d, \quad (90)$$

which holds for every $\varepsilon > 0$ and its existing δ that were defined above.

Note that using $|o(\|\mathbf{x} - \mathbf{x}_i\|_2)| < \|\mathbf{x} - \mathbf{x}_i\|_2$ in (87) requires that $\|\mathbf{x} - \mathbf{x}_i\|_2 \in (0, \delta)$ for any $\mathbf{x} \in A_i$ (i.e., over the entire integrated region). This implies, using (88) for $k = 1$, that

$$\begin{aligned} V(A_i)^{1+\frac{1}{d}} &= \frac{1}{M_1(A_i) \cdot d} \int_{\mathbf{x} \in A_i} \|\mathbf{x} - \mathbf{x}_i\|_2 d\mathbf{x} \\ &< \frac{1}{M_1(A_i) \cdot d} \int_{\mathbf{x} \in A_i} \delta d\mathbf{x} = \frac{1}{M_1(A_i) \cdot d} V(A_i) \delta \end{aligned} \quad (91)$$

and therefore

$$V(A_i) < \left(\frac{\delta}{M_1(A_i) \cdot d} \right)^d. \quad (92)$$

Hence, (90) proves (86).

Let us return to (83) to further develop it,

$$c_i^{\text{opt}} = \frac{p_{\mathbf{x}}(\mathbf{x}_i) V(A_i) \left(\beta(\mathbf{x}_i) + o\left(V(A_i)^{\frac{1}{d}}\right) \right)}{p_{\mathbf{x}}(\mathbf{x}_i) V(A_i) \left(1 + o\left(V(A_i)^{\frac{1}{d}}\right) \right)} = \frac{\beta(\mathbf{x}_i) + o\left(V(A_i)^{\frac{1}{d}}\right)}{1 + o\left(V(A_i)^{\frac{1}{d}}\right)} \quad (93)$$

$$= \left(1 + o\left(V(A_i)^{\frac{1}{d}}\right) \right) \left(\beta(\mathbf{x}_i) + o\left(V(A_i)^{\frac{1}{d}}\right) \right) \quad (94)$$

$$= \beta(\mathbf{x}_i) + o\left(V(A_i)^{\frac{1}{d}}\right) \quad (95)$$

where (94) is due to the little-o property: if $f(\mathbf{x}) \in o(1)$ then $\frac{1}{1+o(f(\mathbf{x}))} = 1 + o(f(\mathbf{x}))$. By this, we complete the proof of (27) in Theorem 4.

The proof of the error formula (28) in Theorem 4 is by setting the linear approximations (25)-(26) and the optimal constants for small regions (27) in the error formula (7):

$$\mathcal{E}_{\text{test}}(\{A_i\}_{i=1}^m, \{c_i^{\text{opt}}\}_{i=1}^m) = \quad (96)$$

$$\begin{aligned} &= \sigma_{\epsilon}^2 + \sum_{i=1}^m \int_{\mathbf{x} \in A_i} \left(\beta(\mathbf{x}_i) + o\left(V(A_i)^{\frac{1}{d}}\right) - (\beta(\mathbf{x}_i) + \nabla \beta(\mathbf{x}_i)^T (\mathbf{x} - \mathbf{x}_i) + R_{\beta,1}(\mathbf{x})) \right)^2 \\ &\quad \cdot (p_{\mathbf{x}}(\mathbf{x}_i) + \nabla p_{\mathbf{x}}(\mathbf{x}_i)^T (\mathbf{x} - \mathbf{x}_i) + R_{p_{\mathbf{x}},1}(\mathbf{x})) \, d\mathbf{x} \\ &= \sigma_{\epsilon}^2 + \sum_{i=1}^m \int_{\mathbf{x} \in A_i} \left(\nabla \beta(\mathbf{x}_i)^T (\mathbf{x} - \mathbf{x}_i) + R_{\beta,1}(\mathbf{x}) + o\left(V(A_i)^{\frac{1}{d}}\right) \right)^2 \\ &\quad \cdot (p_{\mathbf{x}}(\mathbf{x}_i) + \nabla p_{\mathbf{x}}(\mathbf{x}_i)^T (\mathbf{x} - \mathbf{x}_i) + R_{p_{\mathbf{x}},1}(\mathbf{x})) \, d\mathbf{x} \\ &= \sigma_{\epsilon}^2 + \sum_{i=1}^m \left(o\left(V(A_i)^{1+\frac{2}{d}}\right) + \int_{\mathbf{x} \in A_i} (\nabla \beta(\mathbf{x}_i)^T (\mathbf{x} - \mathbf{x}_i))^2 (p_{\mathbf{x}}(\mathbf{x}_i) + \nabla p_{\mathbf{x}}(\mathbf{x}_i)^T (\mathbf{x} - \mathbf{x}_i)) \, d\mathbf{x} \right) \end{aligned} \quad (97)$$

$$\begin{aligned} &= \sigma_{\epsilon}^2 + \sum_{i=1}^m \left(o\left(V(A_i)^{1+\frac{2}{d}}\right) + p_{\mathbf{x}}(\mathbf{x}_i) \int_{\mathbf{x} \in A_i} (\nabla \beta(\mathbf{x}_i)^T (\mathbf{x} - \mathbf{x}_i))^2 \, d\mathbf{x} \right. \\ &\quad \left. + \int_{\mathbf{x} \in A_i} (\nabla \beta(\mathbf{x}_i)^T (\mathbf{x} - \mathbf{x}_i))^2 (\nabla p_{\mathbf{x}}(\mathbf{x}_i)^T (\mathbf{x} - \mathbf{x}_i)) \, d\mathbf{x} \right). \end{aligned} \quad (98)$$

The detailed proof of the equality (97) is lengthy and therefore omitted here; yet, the proof is based on little-o expressions for various integrals over products of little-o terms and moment of inertia, which are technically similar to other parts of the proof that are explicitly shown in this appendix.

To continue to proof, we use the Cauchy-Schwarz inequality to get

$$(\nabla \beta(\mathbf{x}_i)^T (\mathbf{x} - \mathbf{x}_i))^2 \leq \|\nabla \beta(\mathbf{x}_i)\|_2^2 \|\mathbf{x} - \mathbf{x}_i\|_2^2 \quad (99)$$

$$\nabla p_{\mathbf{x}}(\mathbf{x}_i)^T (\mathbf{x} - \mathbf{x}_i) \leq |\nabla p_{\mathbf{x}}(\mathbf{x}_i)^T (\mathbf{x} - \mathbf{x}_i)| \leq \|\nabla p_{\mathbf{x}}(\mathbf{x}_i)\|_2 \|\mathbf{x} - \mathbf{x}_i\|_2. \quad (100)$$

Therefore, we can upper bound (98) as

$$\begin{aligned} \mathcal{E}_{\text{test}}(\{A_i\}_{i=1}^m, \{c_i^{\text{opt}}\}_{i=1}^m) &\leq \sigma_\epsilon^2 + \sum_{i=1}^m \left(o\left(V(A_i)^{1+\frac{2}{d}}\right) + p_{\mathbf{x}}(\mathbf{x}_i) \|\nabla \beta(\mathbf{x}_i)\|_2^2 \int_{\mathbf{x} \in A_i} \|\mathbf{x} - \mathbf{x}_i\|_2^2 d\mathbf{x} \right. \\ &\quad \left. + \|\nabla \beta(\mathbf{x}_i)\|_2^2 \|\nabla p_{\mathbf{x}}(\mathbf{x}_i)\|_2 \int_{\mathbf{x} \in A_i} \|\mathbf{x} - \mathbf{x}_i\|_2^3 d\mathbf{x} \right). \end{aligned} \quad (101)$$

The definition of the normalized second-moment of inertia (24) implies that

$$\int_{\mathbf{x} \in A_i} \|\mathbf{x} - \mathbf{x}_i\|_2^2 d\mathbf{x} = M(A_i) \cdot d \cdot V(A_i)^{1+\frac{2}{d}}. \quad (102)$$

Using the definition of the normalized k^{th} moment of inertia (88), for $k = 3$, we get

$$\int_{\mathbf{x} \in A_i} \|\mathbf{x} - \mathbf{x}_i\|_2^3 d\mathbf{x} = M_3(A_i) \cdot d \cdot V(A_i)^{1+\frac{3}{d}}. \quad (103)$$

Note that $V(A_i)^{1+\frac{3}{d}} \in o\left(V(A_i)^{1+\frac{2}{d}}\right)$ as $V(A_i) \rightarrow 0$. Therefore,

$$\int_{\mathbf{x} \in A_i} \|\mathbf{x} - \mathbf{x}_i\|_2^3 d\mathbf{x} \in o\left(V(A_i)^{1+\frac{2}{d}}\right). \quad (104)$$

Setting (102) and (104) in (101) gives

$$\begin{aligned} \mathcal{E}_{\text{test}}(\{A_i\}_{i=1}^m, \{c_i^{\text{opt}}\}_{i=1}^m) &\leq \sigma_\epsilon^2 + \sum_{i=1}^m \left(o\left(V(A_i)^{1+\frac{2}{d}}\right) + p_{\mathbf{x}}(\mathbf{x}_i) \|\nabla \beta(\mathbf{x}_i)\|_2^2 M(A_i) \cdot d \cdot V(A_i)^{1+\frac{2}{d}} \right) \end{aligned} \quad (105)$$

$$= \sigma_\epsilon^2 + d \sum_{i=1}^m \left(p_{\mathbf{x}}(\mathbf{x}_i) \|\nabla \beta(\mathbf{x}_i)\|_2^2 M(A_i) V(A_i)^{1+\frac{2}{d}} \right) + o\left(V_{\max}^{1+\frac{2}{d}}\right) \quad (106)$$

where $V_{\max} = \max_{i \in \{1, \dots, m\}} V(A_i)$. This concludes the proof of Theorem 4.

F.2. Additional Details on Corollary 5

Starting from the test error formula (28), we omit the explicit inaccuracy term $o\left(V_{\max}^{1+\frac{2}{d}}\right)$ and develop as follows:

$$\begin{aligned}\mathcal{E}_{\text{test}} \leq \mathcal{E}_{\text{test}}^{\text{bound}} &\approx \sigma_{\epsilon}^2 + d \sum_{i=1}^m p_{\mathbf{x}}(\mathbf{x}_i) \|\nabla \beta(\mathbf{x}_i)\|_2^2 M(A_i) V(A_i)^{1+\frac{2}{d}} \quad (107) \\ &\approx \sigma_{\epsilon}^2 + d \sum_{i=1}^m p_{\mathbf{x}}(\mathbf{x}_i) \|\nabla \beta(\mathbf{x}_i)\|_2^2 \mu(\mathbf{x}_i) \frac{1}{m^{2/d} \lambda^{2/d}(\mathbf{x}_i)} V(A_i) \\ &\approx \sigma_{\epsilon}^2 + \frac{d}{m^{2/d}} \int_{\mathbf{x} \in [0,1]^d} \frac{\|\nabla \beta(\mathbf{x})\|_2^2 p_{\mathbf{x}}(\mathbf{x}) \mu(\mathbf{x})}{\lambda^{2/d}(\mathbf{x})} d\mathbf{x} \\ &\triangleq \tilde{\mathcal{E}}_{\text{test}}^{\text{bound}}\end{aligned}$$

where $\mu(\mathbf{x})$ is a smooth moment of inertia profile from Assumption 3. The developments in (107) use Assumptions 2-3 and approximation of the sum as integral due to the small region assumption.

F.3. Proof of Theorem 13: The Optimal Expert Segment Density and the Corresponding Test Error in the Multidimensional Case

Let us develop a lower bound for the integral $\int_{\mathbf{x} \in [0,1]^d} \frac{\|\nabla \beta(\mathbf{x})\|_2^2 p_{\mathbf{x}}(\mathbf{x})}{\lambda^{2/d}(\mathbf{x})} d\mathbf{x}$ from the test error upper bound formula of Corollary 12. This will lead to the segment density that minimizes the test error upper bound. By Hölder's inequality,

$$\begin{aligned}\left(\int_{\mathbf{x} \in [0,1]^d} \left(\left(\|\nabla \beta(\mathbf{x})\|_2^2 p_{\mathbf{x}}(\mathbf{x}) \right)^{\frac{d}{d+2}} \frac{1}{\lambda^{\frac{2}{d+2}}(\mathbf{x})} \right)^{\frac{d+2}{d}} d\mathbf{x} \right)^{\frac{d}{d+2}} \left(\int_{\mathbf{x} \in [0,1]^d} \left(\lambda^{\frac{2}{d+2}}(\mathbf{x}) \right)^{\frac{d+2}{2}} d\mathbf{x} \right)^{\frac{2}{d+2}} \\ \geq \int_{\mathbf{x} \in [0,1]^d} \left(\|\nabla \beta(\mathbf{x})\|_2^2 p_{\mathbf{x}}(\mathbf{x}) \right)^{\frac{d}{d+2}} d\mathbf{x} \quad (108)\end{aligned}$$

where the left side can be simplified, thus,

$$\begin{aligned}\left(\int_{\mathbf{x} \in [0,1]^d} \|\nabla \beta(\mathbf{x})\|_2^2 p_{\mathbf{x}}(\mathbf{x}) \frac{1}{\lambda^{2/d}(\mathbf{x})} d\mathbf{x} \right)^{\frac{d}{d+2}} \left(\int_{\mathbf{x} \in [0,1]^d} \lambda(\mathbf{x}) d\mathbf{x} \right)^{\frac{2}{d+2}} \\ \geq \int_{\mathbf{x} \in [0,1]^d} \left(\|\nabla \beta(\mathbf{x})\|_2^2 p_{\mathbf{x}}(\mathbf{x}) \right)^{\frac{d}{d+2}} d\mathbf{x}. \quad (109)\end{aligned}$$

The density $\lambda(\mathbf{x})$ integrates to 1, i.e., $\int_{\mathbf{x} \in [0,1]^d} \lambda(\mathbf{x}) d\mathbf{x} = 1$, hence, we get that

$$\int_{\mathbf{x} \in [0,1]^d} \|\nabla \beta(\mathbf{x})\|_2^2 p_{\mathbf{x}}(\mathbf{x}) \frac{1}{\lambda^{2/d}(\mathbf{x})} d\mathbf{x} \geq \left(\int_{\mathbf{x} \in [0,1]^d} \left(\|\nabla \beta(\mathbf{x})\|_2^2 p_{\mathbf{x}}(\mathbf{x}) \right)^{\frac{d}{d+2}} d\mathbf{x} \right)^{\frac{d+2}{d}} \quad (110)$$

where the left side is the integral from the test error bound formulated in Corollary 12.

Hölder's inequality in (108) is attained with equality if $\lambda(\mathbf{x})$ is linearly proportional to $\|\nabla\beta(\mathbf{x})\|_2^2 p_{\mathbf{x}}(\mathbf{x}) \frac{1}{\lambda^{2/d}(\mathbf{x})}$. Namely, for a constant ζ such that

$$\lambda(\mathbf{x}) = \zeta \cdot \|\nabla\beta(\mathbf{x})\|_2^2 p_{\mathbf{x}}(\mathbf{x}) \frac{1}{\lambda^{2/d}(\mathbf{x})} \quad (111)$$

which, using integration over $[0, 1]^d$ and that the density integrates to 1, implies that

$$\zeta = \frac{1}{\left(\int_{\mathbf{x} \in [0,1]^d} \left(\|\nabla\beta(\mathbf{x})\|_2^2 p_{\mathbf{x}}(\mathbf{x}) \right)^{\frac{d}{d+2}} d\mathbf{x} \right)^{\frac{d+2}{d}}}. \quad (112)$$

Consequently, the density that minimizes the integral in the left side of (110) is

$$\lambda^{\text{UBM}}(\mathbf{x}) = \frac{\left(\|\nabla\beta(\mathbf{x})\|_2^2 p_{\mathbf{x}}(\mathbf{x}) \right)^{\frac{d}{d+2}}}{\int_{\boldsymbol{\xi} \in [0,1]^d} \left(\|\nabla\beta(\boldsymbol{\xi})\|_2^2 p_{\mathbf{x}}(\boldsymbol{\xi}) \right)^{\frac{d}{d+2}} d\boldsymbol{\xi}}. \quad (113)$$

The optimal density $\lambda^{\text{UBM}}(\mathbf{x})$ makes (110) to hold with equality. Then, plugging the right side of (110) into the test error bound formulated in Corollary 12 gives the minimal bound of

$$\tilde{\mathcal{E}}_{\text{test}}^{\text{bound,min}} = \sigma_{\epsilon}^2 + \frac{d \cdot M(A_d^{\text{opt}})}{m^{2/d}} \left(\int_{\mathbf{x} \in [0,1]^d} \left(\|\nabla\beta(\mathbf{x})\|_2^2 p_{\mathbf{x}}(\mathbf{x}) \right)^{\frac{d}{d+2}} d\mathbf{x} \right)^{1+\frac{2}{d}}. \quad (114)$$

This completes the proof of Theorem 13.

Appendix G. Proofs for Section 6

G.1. Proof of Theorem 7: The Learned Constant Expert is Unbiased

By the learned constant formula in (35), the formula for expectation conditioned on an event (here the event is $n_i > 0$), the conditional expectation rule, the independence among $\{q_i^{(j)}\}_{j=1}^n$ for a specific region A_i , and the definition (34) of n_i as the sum of all the variables $\{q_i^{(j)}\}_{j=1}^n$:

$$\begin{aligned} \mathbb{E}[\tilde{c}_i | n_i > 0] &= \frac{\mathbb{E}[\tilde{c}_i \cdot \mathbb{I}[n_i > 0]]}{\text{Prob}[n_i > 0]} = \frac{\mathbb{E}\left[\mathbb{I}[n_i > 0] \cdot \frac{1}{n_i} \sum_{j:q_i^{(j)}=1} y^{(j)}\right]}{\text{Prob}[n_i > 0]} \\ &= \frac{\mathbb{E}_{\{q_i^{(j)}\}_{j=1}^n} \left[\mathbb{I}[n_i > 0] \cdot \frac{1}{n_i} \sum_{j:q_i^{(j)}=1} \mathbb{E}[y^{(j)} | q_i^{(j)} = 1] \right]}{\text{Prob}[n_i > 0]} \end{aligned} \quad (115)$$

where the value of $q_i^{(j)}$ is 1 in the conditional expectation of $y^{(j)}$ in the sum due the condition $j : q_i^{(j)} = 1$ in the summation.

By the training data model (32) and the zero mean of the noise, the inner conditional expectation in (115) can be developed as follows:

$$\mathbb{E} \left[y^{(j)} | q_i^{(j)} \right] = \mathbb{E} \left[\beta \left(\mathbf{x}^{(j)} \right) + \epsilon^{(j)} | q_i^{(j)} \right] = \mathbb{E} \left[\beta \left(\mathbf{x}^{(j)} \right) | q_i^{(j)} \right] + \mathbb{E} \left[\epsilon^{(j)} \right] = \mathbb{E} \left[\beta \left(\mathbf{x}^{(j)} \right) | q_i^{(j)} \right]. \quad (116)$$

Note that $q_i^{(j)}$ is a Bernoulli random variable with

$$\text{Prob} \left[q_i^{(j)} = 1 \right] = \text{Prob} \left[\mathbf{x}^{(j)} \in A_i \right] = \int_{\mathbf{x} \in A_i} p_{\mathbf{x}}(\mathbf{x}) d\mathbf{x}. \quad (117)$$

Then, the expectation of $y^{(j)}$ conditioned on the event $q_i^{(j)} = 1$ is

$$\mathbb{E} \left[y^{(j)} | q_i^{(j)} = 1 \right] = \mathbb{E} \left[\beta \left(\mathbf{x}^{(j)} \right) | q_i^{(j)} = 1 \right] = \frac{\int_{\mathbf{x} \in A_i} \beta(\mathbf{x}) p_{\mathbf{x}}(\mathbf{x}) d\mathbf{x}}{\int_{\mathbf{x} \in A_i} p_{\mathbf{x}}(\mathbf{x}) d\mathbf{x}} = c_i^{\text{opt}} \quad (118)$$

where the last equality is due to the formula of the optimal constant (without small region assumptions) from (9).

Setting (118) back in (115) gives

$$\begin{aligned} \mathbb{E} [\tilde{c}_i | n_i > 0] &= \frac{\mathbb{E} \left\{ q_i^{(j)} \right\}_{j=1}^n \left[\mathbb{I}[n_i > 0] \cdot \frac{1}{n_i} \cdot n_i c_i^{\text{opt}} \right]}{\text{Prob} [n_i > 0]} = \frac{\mathbb{E} \left\{ q_i^{(j)} \right\}_{j=1}^n [\mathbb{I}[n_i > 0]]}{\text{Prob} [n_i > 0]} c_i^{\text{opt}} \\ &= \frac{1 \cdot \text{Prob} [n_i > 0]}{\text{Prob} [n_i > 0]} c_i^{\text{opt}} = c_i^{\text{opt}} \end{aligned} \quad (119)$$

which completes the proof of Theorem 7.

G.2. Proof of Lemma 8

We develop the test error for the learned expert constants, starting from the test error formula of (7):

$$\begin{aligned} \mathcal{E}_{\text{test}} (\{A_i\}_{i=1}^m, \{\tilde{c}_i\}_{i=1}^m) &= \sigma_{\epsilon}^2 + \sum_{i=1}^m \int_{\mathbf{x} \in A_i} (\tilde{c}_i - \beta(\mathbf{x}))^2 p_{\mathbf{x}}(\mathbf{x}) d\mathbf{x} \\ &= \sigma_{\epsilon}^2 + \sum_{i=1}^m \int_{\mathbf{x} \in A_i} (\tilde{c}_i - c_i^{\text{opt}} + c_i^{\text{opt}} - \beta(\mathbf{x}))^2 p_{\mathbf{x}}(\mathbf{x}) d\mathbf{x} \\ &= \sigma_{\epsilon}^2 + \sum_{i=1}^m (\tilde{c}_i - c_i^{\text{opt}})^2 \int_{\mathbf{x} \in A_i} p_{\mathbf{x}}(\mathbf{x}) d\mathbf{x} \\ &\quad + \sum_{i=1}^m \int_{\mathbf{x} \in A_i} (c_i^{\text{opt}} - \beta(\mathbf{x}))^2 p_{\mathbf{x}}(\mathbf{x}) d\mathbf{x} \\ &\quad + 2 \sum_{i=1}^m (\tilde{c}_i - c_i^{\text{opt}}) \int_{\mathbf{x} \in A_i} (c_i^{\text{opt}} - \beta(\mathbf{x})) p_{\mathbf{x}}(\mathbf{x}) d\mathbf{x}. \end{aligned} \quad (120)$$

According to (7), the second sum in (120) is related to test error of MoE with optimal constant experts (for a given routing segmentation) as

$$\sum_{i=1}^m \int_{\mathbf{x} \in A_i} (c_i^{\text{opt}} - \beta(\mathbf{x}))^2 p_{\mathbf{x}}(\mathbf{x}) d\mathbf{x} = \mathcal{E}_{\text{test}} \left(\{A_i\}_{i=1}^m, \{c_i^{\text{opt}}\}_{i=1}^m \right) - \sigma_{\epsilon}^2. \quad (121)$$

Moreover, for the third sum in (120), note that

$$\begin{aligned} \int_{\mathbf{x} \in A_i} (c_i^{\text{opt}} - \beta(\mathbf{x})) p_{\mathbf{x}}(\mathbf{x}) d\mathbf{x} &= c_i^{\text{opt}} \int_{\mathbf{x} \in A_i} p_{\mathbf{x}}(\mathbf{x}) d\mathbf{x} - \int_{\mathbf{x} \in A_i} \beta(\mathbf{x}) p_{\mathbf{x}}(\mathbf{x}) d\mathbf{x} \\ &= \frac{\int_{\mathbf{x} \in A_i} \beta(\mathbf{x}) p_{\mathbf{x}}(\mathbf{x}) d\mathbf{x}}{\int_{\mathbf{x} \in A_i} p_{\mathbf{x}}(\mathbf{x}) d\mathbf{x}} \cdot \int_{\mathbf{x} \in A_i} p_{\mathbf{x}}(\mathbf{x}) d\mathbf{x} - \int_{\mathbf{x} \in A_i} \beta(\mathbf{x}) p_{\mathbf{x}}(\mathbf{x}) d\mathbf{x} \\ &= 0 \end{aligned} \quad (122)$$

where the optimal constant formula (9) is used here. Setting (121) and (122) back in (120) gives

$$\mathcal{E}_{\text{test}} \left(\{A_i\}_{i=1}^m, \{\tilde{c}_i\}_{i=1}^m \right) = \mathcal{E}_{\text{test}} \left(\{A_i\}_{i=1}^m, \{c_i^{\text{opt}}\}_{i=1}^m \right) + \sum_{i=1}^m (\tilde{c}_i - c_i^{\text{opt}})^2 \int_{\mathbf{x} \in A_i} p_{\mathbf{x}}(\mathbf{x}) d\mathbf{x}. \quad (123)$$

Using that, by (10),

$$\mathcal{E}_{\text{app}} \left(\mathcal{H}_{m,d}^c \left(\{A_i\}_{i=1}^m \right) \right) = \mathcal{E}_{\text{test}} \left(\{A_i\}_{i=1}^m, \{c_i^{\text{opt}}\}_{i=1}^m \right),$$

and defining the estimation error, using $\rho_i = \text{Prob} [\mathbf{x} \in A_i] = \int_{\mathbf{x} \in A_i} p_{\mathbf{x}}(\mathbf{x}) d\mathbf{x}$ from (36), as

$$\mathcal{E}_{\text{est}}(m, \mathcal{S}_n) = \sum_{i=1}^m (\tilde{c}_i - c_i^{\text{opt}})^2 \rho_i$$

completes the proof of Lemma 8.

G.3. Proof of Lemma 9

The definition of $q_i^{(j)}$ in (33) implies it is a Bernoulli random variable with probability ρ_i (recall (36)) of $q_i^{(j)} = 1$. Then, definition (34) implies that n_i is a sum of n independent Bernoulli variables $q_i^{(1)}, \dots, q_i^{(n)}$.

A version of the Chernoff bound for a sum of independent Bernoulli variables (Vershynin, 2018) can be written here as

$$\text{for } \tau \in (0, 1), \text{ Prob} [n_i \leq (1 - \tau) \mathbb{E} [n_i]] \leq \exp \left(-\frac{\tau^2 \mathbb{E} [n_i]}{2} \right). \quad (124)$$

According to (33), (34), (36), we have

$$\mathbb{E} [n_i] = n \rho_i \quad (125)$$

and therefore (124) becomes

$$\text{for } \tau \in (0, 1), \text{ Prob}[n_i \leq (1 - \tau)n\rho_i] \leq \exp\left(-\frac{\tau^2 n \rho_i}{2}\right). \quad (126)$$

Upper bounding the right-side probability in (126) with $\tilde{\delta} \in (0, 1)$ yields the condition

$$n \geq \frac{2}{\tau^2 \rho_i} \ln\left(\frac{1}{\tilde{\delta}}\right). \quad (127)$$

Then, setting $\tau = \frac{1}{2}$ in (126) and (127) gives that for $\tilde{\delta} \in (0, 1)$ and $n \geq \frac{8}{\rho_i} \ln\left(\frac{1}{\tilde{\delta}}\right)$

$$\text{Prob}\left[n_i \leq \frac{1}{2}n\rho_i\right] \leq \tilde{\delta}. \quad (128)$$

The inequality in (128) is equivalent to $\text{Prob}[n_i > \frac{1}{2}n\rho_i] \geq 1 - \tilde{\delta}$ and therefore the proof of Lemma 9 is completed.

G.4. Proof of Theorem 10

According to (35), \tilde{c}_i is an average of n_i independent random variables $\{y^{(j)}\}_{j:q_i^{(j)}=1}$. Therefore, conditioned on $n_i = \theta_i$ where $\theta_i \in \{1, \dots, n\}$ is a non-random value, the probability distribution of the random variable \tilde{c}_i is the same as the probability distribution of the random variable

$$\frac{1}{\theta_i} \sum_{\tau=1}^{\theta_i} z_i^{(\tau)} \quad (129)$$

where $z_i^{(1)}, \dots, z_i^{(\theta_i)}$ are i.i.d. drawn from the distribution of $y|\{q_i = 1\}$, such that (\mathbf{x}, y) are drawn from the distribution of the data model (1) and $q_i = \mathbb{I}[\mathbf{x} \in A_i]$.

We use the following assumptions in addition to the data model (1): The function β is bounded on its entire domain. For the i^{th} region A_i , denote the value range size as $R_{\beta,i} \triangleq \max_{\mathbf{x} \in A_i} \beta(\mathbf{x}) - \min_{\mathbf{x} \in A_i} \beta(\mathbf{x})$. The noise ϵ is from the bounded range $[\epsilon_{\min}, \epsilon_{\max}]$. Denote $R_{\epsilon} \triangleq \epsilon_{\max} - \epsilon_{\min}$. Then, for j such that $q_i^{(j)} = 1$, the random variable $y^{(j)}$ gets its value from the range

$$\left[\min_{\mathbf{x} \in A_i} \beta(\mathbf{x}) + \epsilon_{\min}, \max_{\mathbf{x} \in A_i} \beta(\mathbf{x}) + \epsilon_{\max} \right]. \quad (130)$$

The random variables $z_i^{(1)}, \dots, z_i^{(\theta_i)}$ are also from the value range (130).

Then, for $\gamma \geq 0$ and $\theta \in \{1, \dots, n\}$,

$$\begin{aligned} \text{Prob}[|\tilde{c}_i - \mathbb{E}[\tilde{c}_i|n_i = \theta_i]| \geq \gamma | n_i = \theta_i] &= \text{Prob}\left[\left|\frac{1}{\theta_i} \sum_{\tau=1}^{\theta_i} z_i^{(\tau)} - \frac{1}{\theta_i} \mathbb{E}\left[\sum_{\tau=1}^{\theta_i} z_i^{(\tau)}\right]\right| \geq \gamma\right] \\ &\leq 2 \exp\left(-\frac{2\gamma^2 \theta_i}{(v_{\max,i} - v_{\min,i})^2}\right) \end{aligned} \quad (131)$$

where the last inequality is due to Hoeffding's inequality; by (130), $v_{\max,i} = \max_{\mathbf{x} \in A_i} \beta(\mathbf{x}) + \epsilon_{\max}$ and $v_{\min,i} = \min_{\mathbf{x} \in A_i} \beta(\mathbf{x}) + \epsilon_{\min}$, therefore,

$$v_{\max,i} - v_{\min,i} = R_{\beta,i} + R_{\epsilon}. \quad (132)$$

Recall that, according to Theorem 7, $\mathbb{E} [\tilde{c}_i | n_i > 0] = c_i^{\text{opt}}$. It can be proved similarly to Appendix G.1 that

$$\mathbb{E} [\tilde{c}_i | n_i = \theta_i] = c_i^{\text{opt}}, \quad \text{for } \theta_i \in \{1, \dots, n\}. \quad (133)$$

Then, setting (133) in (131) gives

$$\text{Prob} [|\tilde{c}_i - c_i^{\text{opt}}| \geq \gamma | n_i = \theta_i] \leq 2 \exp \left(-\frac{2\gamma^2 \theta_i}{(v_{\max,i} - v_{\min,i})^2} \right). \quad (134)$$

Let us extend the conditioning such that $n_i \geq \eta_i$, i.e., $n_i \in \{\lceil \eta_i \rceil, \dots, n\}$ where η_i is a positive non-random value from the continuous range $(0, n]$:

$$\text{Prob} [|\tilde{c}_i - c_i^{\text{opt}}| \geq \gamma | n_i \geq \eta_i] = \frac{\text{Prob} [|\tilde{c}_i - c_i^{\text{opt}}| \geq \gamma, n_i \geq \eta_i]}{\text{Prob} [n_i \geq \eta_i]} \quad (135)$$

$$= \frac{\sum_{\theta_i=\lceil \eta_i \rceil}^n \text{Prob} [|\tilde{c}_i - c_i^{\text{opt}}| \geq \gamma | n_i = \theta_i] \text{Prob} [n_i = \theta_i]}{\text{Prob} [n_i \geq \eta_i]} \quad (136)$$

$$\leq \frac{\sum_{\theta_i=\lceil \eta_i \rceil}^n 2 \exp \left(-\frac{2\gamma^2 \theta_i}{(v_{\max,i} - v_{\min,i})^2} \right) \text{Prob} [n_i = \theta_i]}{\text{Prob} [n_i \geq \eta_i]} \quad (137)$$

$$\leq \frac{2 \exp \left(-\frac{2\gamma^2 \eta_i}{(v_{\max,i} - v_{\min,i})^2} \right) \sum_{\theta_i=\lceil \eta_i \rceil}^n \text{Prob} [n_i = \theta_i]}{\text{Prob} [n_i \geq \eta_i]} \quad (138)$$

$$= \frac{2 \exp \left(-\frac{2\gamma^2 \eta_i}{(v_{\max,i} - v_{\min,i})^2} \right) \text{Prob} [n_i \geq \eta_i]}{\text{Prob} [n_i \geq \eta_i]} \quad (139)$$

$$= 2 \exp \left(-\frac{2\gamma^2 \eta_i}{(v_{\max,i} - v_{\min,i})^2} \right). \quad (140)$$

where the bound in (137) is due to (134), and (139) is due to $\text{Prob} [n_i \geq \eta_i] = \sum_{\theta_i=\lceil \eta_i \rceil}^n \text{Prob} [n_i = \theta_i]$; also, $\text{Prob} [n_i \geq \eta_i] > 0$ due to the assumption that $\rho_i > 0$. Hence, we got

$$\text{Prob} [|\tilde{c}_i - c_i^{\text{opt}}| \geq \gamma | n_i \geq \eta_i] \leq 2 \exp \left(-\frac{2\gamma^2 \eta_i}{(v_{\max,i} - v_{\min,i})^2} \right) \quad (141)$$

The concentration inequality (141) can be equivalently written as follows. For $\eta_i \in (0, n]$, $\gamma \geq 0$,

$$\text{Prob} \left[\left| \tilde{c}_i - c_i^{\text{opt}} \right| \geq \gamma \frac{R_{\beta,i} + R_{\epsilon}}{\sqrt{2\eta_i}} \middle| n_i \geq \eta_i \right] \leq 2 \exp (-\gamma^2). \quad (142)$$

Put differently, for $\gamma \geq 0$, $\eta_i \in (0, n]$, and given $n_i \geq \eta_i$,

$$|\tilde{c}_i - c_i^{\text{opt}}| < \gamma \frac{R_{\beta,i} + R_\epsilon}{\sqrt{2\eta_i}} \quad (143)$$

with probability at least $1 - 2 \exp(-\gamma^2)$.

Recall that this theorem assumes $\rho_i > 0$. Then, from Lemma 9, for $\tilde{\delta} \in (0, 1)$ and given $n \geq \frac{8}{\rho_i} \ln\left(\frac{1}{\tilde{\delta}}\right)$, we have $n_i > \frac{1}{2}n\rho_i$ with probability at least $1 - \tilde{\delta}$.

Hence, the probabilistic intersection of (143) for $\eta_i = \frac{1}{2}n\rho_i$ and Lemma 9 gives that for $\gamma \geq 0$, $\tilde{\delta} \in (0, 1)$ and given $n \geq \frac{8}{\rho_i} \ln\left(\frac{1}{\tilde{\delta}}\right)$,

$$|\tilde{c}_i - c_i^{\text{opt}}| < \gamma \frac{R_{\beta,i} + R_\epsilon}{\sqrt{n\rho_i}} \quad (144)$$

with probability at least $1 - 2 \exp(-\gamma^2) - \tilde{\delta}$. This completes the proof.

G.5. Proof of Theorem 11

The proof starts from the estimation error formula (39) of Lemma 8 and setting into it the upper bound of $|\tilde{c}_i - c_i^{\text{opt}}|$ from Theorem 10:

$$\mathcal{E}_{\text{est}}(m, \mathcal{S}_n) = \sum_{i=1}^m (\tilde{c}_i - c_i^{\text{opt}})^2 \rho_i \quad (145)$$

$$< \sum_{i=1}^m \left(\gamma \frac{R_{\beta,i} + R_\epsilon}{\sqrt{n\rho_i}} \right)^2 \rho_i \quad (146)$$

$$\begin{aligned} &= \frac{\gamma^2}{n} \sum_{i=1}^m (R_{\beta,i} + R_\epsilon)^2 \\ &\leq \frac{\gamma^2}{n} m \cdot \max_{i \in \{1, \dots, m\}} (R_{\beta,i} + R_\epsilon)^2 \end{aligned}$$

The inequality in (146) is due to applying Theorem 10 to upper bound $|\tilde{c}_i - c_i^{\text{opt}}|$ each of the m experts in the sum. These m applications of Theorem 10 are for the same $\gamma > 0$ and $\tilde{\delta} \in (0, 1)$. For each of the m experts, the upper bound for $|\tilde{c}_i - c_i^{\text{opt}}|$ holds with probability at least $1 - 2 \exp(-\gamma^2) - \tilde{\delta}$; hence, the upper bounds hold for all the m experts with probability at least $1 - 2m \exp(-\gamma^2) - m\tilde{\delta}$.